Analysis of Fluorescent Microscopy Images to Better Understand Keratin's Effect on Protein Recycling Pathways in Human Embryonic Kidney Cells

An Undergraduate Thesis Presented to the
Faculty of the Department of Biology

Western Carolina University
Cullowhee, North Carolina

In Partial Fulfillment
of the Requirements for the Degree
Bachelor of Science

Bailey Trumm

Advisor: Heather B. Coan, Ph.D.

Committee: Robert Youker, Ph.D. and André Velásquez, Ph.D.

Table of Contents

Abstract

Protein recycling pathways and autophagy play an important role in maintaining cellular homeostasis, but these processes are also essential for cell survival during times of stress. Protein recycling pathways, such as the ubiquitin-proteasome system (UPS), are important as old, damaged, or non-functional proteins are degraded, and the resulting free amino acids can be used to synthesize new, functional proteins. The process of autophagy works to ensure cellular homeostasis by degrading old or damaged macromolecules into their monomer parts so that they can be recycled to make new materials. Fluorescent microscopy can be used to track these pathways in a lab to inform our understanding of conditions that promote cell recycling in times of stress. However, the Coan laboratory has had difficulty standardizing image analysis using fluorescent microscopy. Counting of fluorescent image data to obtain quantitative comparisons for our lab's cell recycling and biomaterial studies has demonstrated that manual counting is subjective and prone to error. Therefore, this study aimed to investigate the usability and reliability of images obtained via fluorescence microscopy techniques that are commonly used to investigate these pathways. In this study, I compiled data from past experiments for reanalysis with a goal of determining 1) whether these data can be replicated when reanalyzed (manually counted) and 2) whether we can glean new information from the dataset through manual counts of a parameter not previously analyzed. The results suggest that manual counting of fluorescent images can be standardized, but great care must be taken to ensure that high quality images are taken during experiments and that each manual count must follow a defined protocol. I also found that a new analysis of data may yield important results previously overlooked in our laboratory.

Background and Introduction

Keratin Biomaterials in the Coan Lab

Biomaterials are extensively used and extremely important in modern science and medicine. Biomaterials can be natural or synthetic, and are used to support, enhance, or replace damaged tissues or bodily functions [1]. There are several different types of biomaterials- and these have a variety of functions- such as aiding in drug delivery, promoting healing or regeneration of tissues, use as a scaffold on which cells can attach and proliferate, serving as a medical implant, and acting as molecular probes or biosensors [1]. A good biomaterial is one that is biocompatible, naturally abundant, mechanically compatible, and wear resistant [2], and biomaterials can be made from metals, plastic, ceramics, glass, and from living cells and tissues [1]. An example of a natural, protein-derived biomaterial is keratin. Keratins are a family of intermediate filament proteins produced and found in vertebrate epithelia such as hair, nails, hooves, wool, and horns [3][4]. Keratin extracted from human hair has been found to serve as a good biomaterial for many reasons: it is derived from humans and demonstrates biocompatibility, it is biodegradable, it does not cause a strong immune response when inserted into human tissue, and, unlike some difficult to obtain biomaterials, it is readily available in large quantities [5]. Research of human keratins has led to the discovery and classification of 54 different keratin genes [6]. Initially, the term “keratin” more generally described the group of insoluble proteins that link as intermediate filament proteins that are abundant in the cytoplasm of epithelial cells and various epidermal appendages like hair, wool, and nails. Further investigation of these proteins led to the categorization of mammalian keratins into two distinct groups based on their structural characteristics, functions, and regulatory mechanism: “hard” and “soft” keratins [7]. The keratins found in human hair are known as hard keratins, and these hard

keratins are made up of 400-600 amino acids, specifically characterized by their high cysteine content, low glycine content, and structural strength [5]. Though hard and soft keratins are very similar in secondary structure, the hard keratins found in human hair are much stronger as they contain significantly more cysteine residues and can therefore form more disulfide bonds [4]. Because of the biological structure and characteristics of keratin, it can act as a successful biomaterial in a variety of ways. Human hair keratins have been shown to possess cell binding motifs that can support cellular attachment, such as leucine-aspartic acid-valine (LDV) and glutamic acid-aspartic acid-serine (EDS) binding residues [4]. It has also been found that keratins can directly influence cell behavior and have regulatory functions such as playing a role in the stress response, apoptosis, and wound healing via intracellular signaling pathways [6]. Our lab and others have found that keratin may have the ability to directly or indirectly influence the autophagy process and the ubiquitin-proteasome system (UPS) [8]. Studies by Poranki et al. show up-regulation of autophagy genes in keratin exposed cells [8][9]. Also, keratinocytes (keratin producing cells of the epidermis) use autophagy as a means by which to respond to wound healing —which might suggest an interaction with keratin proteins and the process [7]. Both autophagy and the UPS are intracellular quality control mechanisms responsible for maintaining homeostasis; however, autophagy is a process that can degrade and recycle many different intracellular components, while the UPS has only one function— to degrade and recycle short-lived, aggregated, and soluble proteins [10]. During times of stress, both autophagy and the UPS are involved in clearing intracellular protein aggregates (made up of damaged or unfolded proteins), and failure to efficiently eliminate these protein aggregates can lead to the cell undergoing apoptosis and death [11]. For both protein clearing mechanisms, ubiquitin serves as a molecular label that is tagged onto these faulty proteins, signaling for them to be degraded [10]

[11]. It is thought that if keratin can in fact influence these protein recycling systems, cells grown on keratin biomaterials could recover quicker from stress. This makes keratin a particularly attractive biomaterial for tissue engineering strategies aimed at regrowing or replacing damaged tissue. A material that can alleviate cell stress or prime cells to better respond to stress could protect newly implanted cells, which commonly die off due to localized inflammation and stress at the implantation site.

Autophagy

Autophagy is a natural process that can differ in various cell types to ensure cell homeostasis. However, autophagy is also a process that is upregulated in response to cellular stress or nutrient deprivation, in which cells degrade and recycle unneeded or damaged components to ensure cell survival. Autophagy can degrade nonfunctional proteins, macromolecules, bacteria, protein aggregates, and damaged organelles (such as mitochondria), and if stressed cells do not undergo autophagy and break down and recycle the biologically active monomers to make new, functional molecules, the cells can die due to nutrient shortage [12][13]. The autophagy process allows the cell to operate more efficiently both in regular maintenance and during times of stress, as protein quality control is a central element for maintaining cell homeostasis. When cells initiate autophagy, materials to be degraded are surrounded by a vesicle called an autophagosome. The autophagosome then merges with the cellular digestive organelle, the lysosome, to form a larger vesicle known as the autophagolysosome. The old or damaged cellular components are broken down by the acidic environment and hydrolytic enzymes of the lysosome, and the reusable materials are recycled to make new cellular components [14].

To investigate the autophagy pathway, a positive control is important so that we understand what changes might occur in cells that are undergoing autophagy. Rapamycin is a commonly used inducer of autophagy that can be used for this purpose (see Figure 1 below). As autophagy is a highly conserved cellular process, it is regulated by several important signal transduction pathways. One such pathway involves the mammalian target of rapamycin (mTOR), a serine/threonine kinase that plays a key role in controlling catabolic processes that promote autophagy. Rapamycin, an inhibitor of mTOR, induces autophagy by inhibiting mTORC1, a component of the mTOR complex. Previous studies have demonstrated that rapamycin induces autophagy in a time- and concentration-dependent manner in various cell types, including HeLa and neuroblastoma cells. HEK293 cells are commonly used in autophagy research, and rapamycin serves as a valuable positive control in such studies for its reliable induction of autophagy [15].

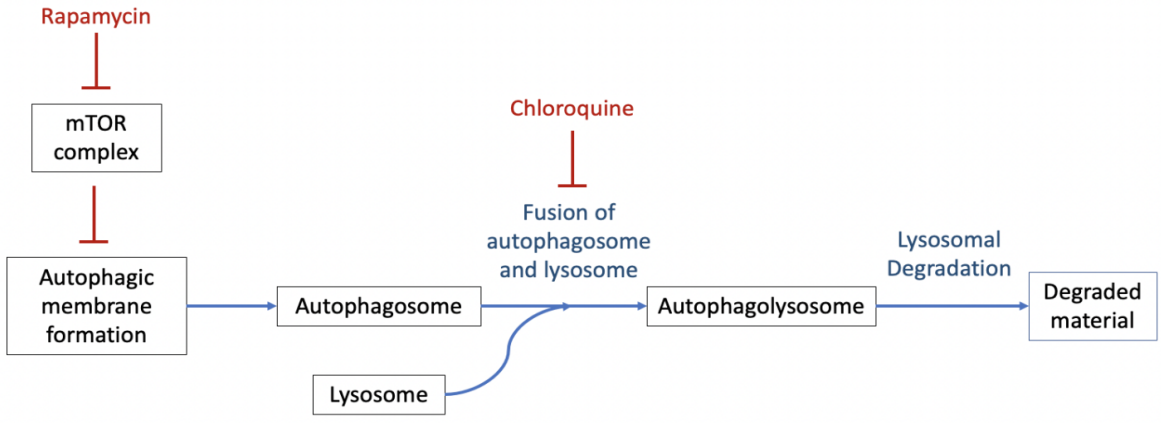

Figure 1. The mechanism in which rapamycin acts as an inducer of autophagy [figure modified from 15].

There are various methods to visualize and study the autophagy process, including gene expression, western blotting, and tracking fluorescently tagged autophagy proteins. In our lab,

we specifically track the fluorescently labeled Light Chain 3 (LC3) protein—a protein specific to autophagy (see Figure 2 below). Using this method, HEK293 cells are transfected with a dual reporter plasmid system containing the LC3 gene fused to two genes that code for fluorescent reporters: Green Fluorescent Protein (GFP) and mCherry, a red fluorescent protein (RFP). (pBABE-puro mCherry-EGFP-LC3B was a gift from Jayanta Debnath [Addgene plasmid #22418; http://n2t.net/addgene:22418;RRID:Addgene_22418]). The cells will then produce an abundance of LC3 proteins tagged with the two reporters post transfection. Before inducing autophagy, the red and green signal is dispersed evenly throughout the cytoplasm as LC3 is expressed and present throughout the cytosol of the cell. After autophagy has been initiated, the LC3 protein is modified and recruited to the autophagosome in high numbers, which can be visualized under a fluorescent microscope as small, intense regions of fluorescence called "puncta." In early autophagy, both green and red puncta can be seen with fluorescence microscopy. As the process continues, the cell's lysosome will fuse with the autophagosome, forming an autophagolysosome, and subsequently degrade the engulfed material. In late autophagy and in the highly acidic environment of the autophagolysosome, the GFP reporter protein (with a pKa of 6.0) becomes nonfunctional and as a result no green fluorescence is observed anymore. The mCherry has a pKa of <4.5, so it remains functional in the acidic environment and continues to display red fluorescence. This is how late autophagy can be identified in cells as only red puncta will be observed. Our LC3 transfection system is useful in tracking the progression of autophagy in cells. When there is little to no autophagy occurring, there will be diffuse green and red fluorescence throughout the cell, in early autophagy there will be clear green and red puncta that can be overlaid to show both in the same cellular location, while in late autophagy only red puncta will be visible [15].

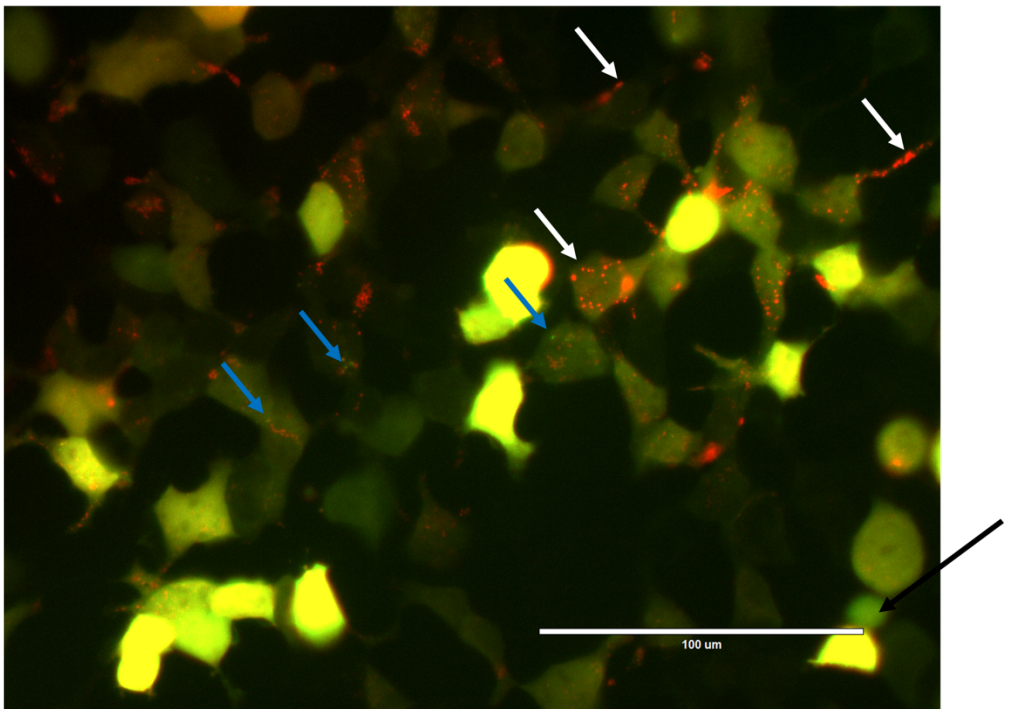

Figure 2. The image highlights how the LC3 Dual Reporter System is used to track autophagy. Blue arrows: point to yellow puncta indicating green/red overlaid fluorescence which suggests the presence of an autophagosome prior to lysosome fusion. White arrows: point to red puncta which show the presence of an autophagolysosome (late autophagy); GFP is pH sensitive and acidic conditions of lysosome prevent fluorescence, so only red is visible following autophagolysosome formation. Black arrow: points to a cell showing diffuse fluorescence (not undergoing autophagy). The white scale represents 100 μm.

Ubiquitin-Proteasome System (Protein Aggregation)

Another cellular response to stress, and the most common method of cytosolic protein degradation overall in eukaryotes, is the activation of the ubiquitin-proteasome system (UPS) [12]. While protein degradation is always happening in cells and is integral to maintaining cellular homeostasis, faulty or damaged proteins due to stress are quickly recognized and degraded [8]. In response to environmental stimuli such as heat stress, proteins can become misfolded or unfolded, and these proteins need to be degraded or refolded to not cause the cell further damage. The UPS is different from autophagy as this process is specifically for degrading proteins (and not other macromolecules), and that the lysosome is not involved. Protein degradation due to the

UPS in eukaryotic cells uses ubiquitin to tag proteins, both cytosolic and nuclear, for proteolysis (Figure 3). There are three enzymes responsible for transferring ubiquitin onto the target protein, known as E1, E2, and E3. E1, the ubiquitin activating enzyme, transfers ubiquitin to the carrier enzyme, E2; E2 then works with the E3 enzymes to tag the protein substrate with ubiquitin [11][12]. Ubiquitin attaches onto the side chain of a lysine residue, and when a protein becomes polyubiquitinated, the 26S proteasome recognizes such tagged protein and degrades it [8]. The cell can recycle and reuse these resulting free amino acids to construct new, improved functioning proteins.

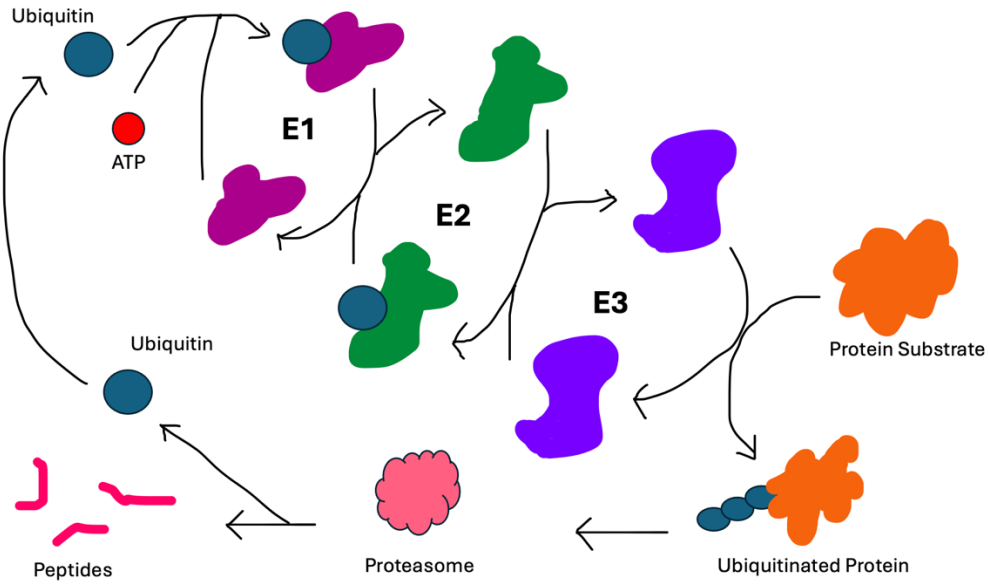

Figure 3. The UPS pathway modified from an image created by Myra Zerr [21].

The Coan lab uses a transfection system to track the UPS system. Specifically, we use the protein chimera GFP-250 as cells overexpressing GFP-250 form protein aggregates, and this is positively correlated with recruitment of the proteasome to eliminate these aggregates via the

UPS [16]. With this system, we induce production of GFP-250 in human cells and exposed these cells to heat shock followed by a recovery period. We then track accumulation and clearance of protein aggregates (via fluorescent microscopy) pre-heat shock, post-heat shock, and during a defined recovery time period (Figure 4).

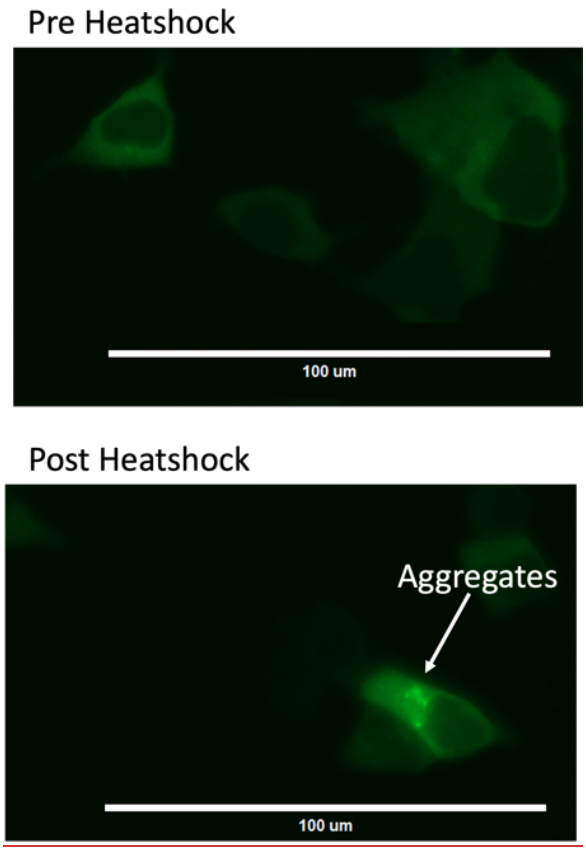

Figure 4. GFP-250 system used to monitor if the UPS system is overwhelmed in our laboratory. The white scale represents 100 μm.

Keratin Biomaterials and Cell Recycling Pathways

The Coan lab has preliminary data to suggest that keratin biomaterials may interact with both of these cellular recycling pathways (autophagy and protein aggregation); however, until we tease apart the details of what is occurring, we don't know whether keratin is interacting with one pathway and indirectly impacting the other, or if it is interacting with both pathways.

Previous studies in our lab investigated the effect of keratin supplements in heat stressed cells [15][17]. The data collected suggest that cells supplemented with keratin clear aggregates more rapidly than those without keratin supplements. Previous studies of keratin treated, starved, and heat shocked cells also suggest a potential relationship between keratin and autophagy—although these studies are less definitive because the transfection system used to track autophagy activation in our lab results in images that are not as easy to interpret as those obtained in aggregate studies.

To better understand keratin's role in these two pathways, I made use of the extensive catalog of past images obtained by the Coan laboratory using these transfection systems. Related to the UPS protein aggregation pathway, I first re-analyzed previously analyzed images to determine the extent to which image data can be replicated by a different user. Second, I analyzed the data with new parameters to determine whether patterns from previous studies could be identified via a different counting technique. In previous studies, aggregate tracking data only focused on the total number of cells with and without aggregates within a field of view over a defined duration of time after heat shock. I further analyzed these images to understand whether there is also a relationship between keratin and the number of aggregates that form within a cell when exposed to heat shock and subsequent recovery. Autophagy studies in our lab utilize a transfection system that allows us to count cells with autophagy vesicles. Different fluorescent reporters correspond to either early or late autophagy. However, these images have only been used to obtain qualitative data due to the difficulty inherent in counting vesicle presence (see Figure 5 below). To this end, I conducted an extensive analysis of formerly obtained image sets to investigate the reliability of using these images. I selected images from cells exposed only to the positive control, rapamycin, known to induce changes within our

experimental system (confirmed via Western Blot in our prior lab studies). Previous assessments lacked detailed manual counts due to the complexity of the data. Taking on this challenge, I aimed to assess the feasibility of using these images to accurately identify autophagy in HEK293 cells, despite their inherent complexity.

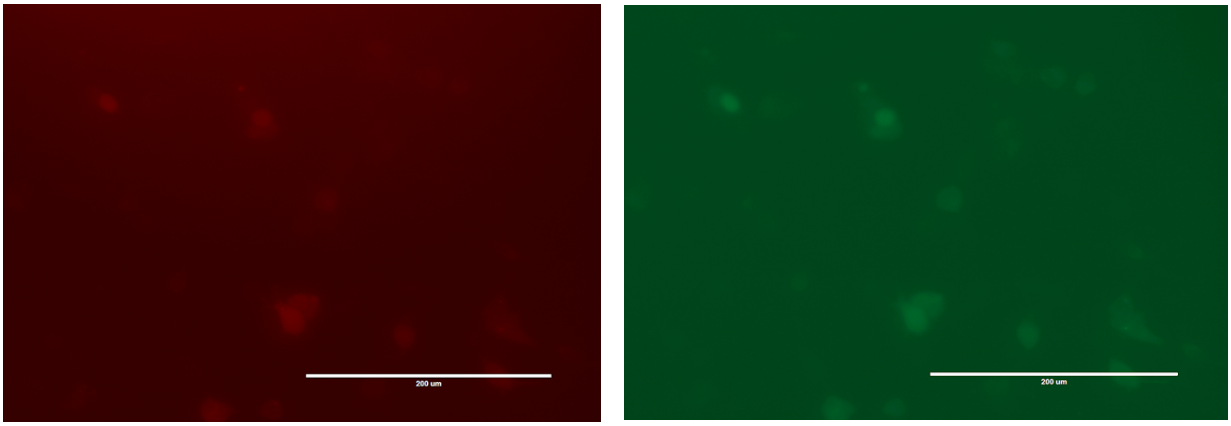

Figure 5. Cells transfected with the LC3 autophagy-tracking plasmid viewed under two different light cubes (Texas Red and Green Fluorescent Protein (GFP)). Red and Green fluorescing proteins are linked to autophagy protein LC3 and the two probes can help differentiate timing of the autophagy process. Diffuse red/green in a cell indicates no autophagy. Bright intense red and green puncta at the same location indicate early autophagy (autophagosome formation). Red only puncta at a location indicates late autophagy. The white scale represents 200 μm.

Specific Aims: For the reasons outlined above, my project consisted of two aims that are detailed here:

AIM 1: I analyzed Human Embryonic Kidney Cell 293 (HEK293) heat shock aggregate formation and clearance data to investigate whether keratin impacts not only clearance of aggregates but also the formation of multiple aggregates within cells.

Sub-Aim I: I reproduced analysis of previous images obtained in the aggregation experiments to confirm that keratin affects aggresome formation and clearance, particularly within the first 30 minutes after heat shock (C. Davis and R. Gardner) [18][19].

Sub-Aim II: I analyzed images to count the number of aggregates per cell throughout the time period in question.

AIM 2: I performed manual counts of the autophagy experimental images as a quantitative method of assessing autophagy activation by rapamycin in HEK cells transfected with the autophagy-reporter plasmid.

Sub-Aim I: The percentage of cells containing puncta was recorded for all images in both light channels. It was hypothesized that over the course of the autophagy process, the difference in these values between the green and red channels would allow us to numerically measure early and late autophagy.

Sub-Aim II: I counted the number of puncta found in each cell throughout the autophagy process. We hypothesized that the number of multiple puncta per cell would increase in rapamycin-treated cells and could be a determinant of autophagy induction.

Materials and Methods

Images that my proposed research analyzed were taken using different transfection systems that allowed us to track aggregate formation and autophagy activation. These images were obtained by other student researchers in Dr. Coan's lab. However, methods used to generate these images are provided here as the methods are important for full understanding of my proposed research. A description of both systems used follows.

HEK293 cell growth and maintenance

HEK293 cells (a gift from Dr. Robert Youker, WCU) were grown and maintained on tissue culture plates in 10% Fetal Bovine Serum (FBS)/Dulbecco's Modified Eagle Medium (DMEM) (Gibco Ref. # 11995-065). Cells were grown under standard conditions in 37°C in 5% CO_2 within a HERA cell humidified incubator. Cell experiments ewer performed by seeding at a uniform density. A hemocytometer was used to obtain cell counts with Trypan Blue dyed cells excluded to avoid counting dead cells. Six-well dishes were used for all experiments and seeded at a density of 150,000 cells/mL.

Transfection of HEK cells for aggregate tracking studies

Aggresome formation in response to heat shock was investigated in HEK293 cells with and without keratin (provided as a gift by Dr. Mark Van Dyke, University of Arizona). HEK293 cells were grown at 37°C and transfected with a plasmid encoding a model GFP-tagged misfolded protein (GFP-250, a gift from Dr. Robert Youker, WCU). Transfection was achieved using OptiMem medium, TurboFect lipids (ThermoFisher), and 250ng/well of plasmid. Two hours prior to heat shock, 0.1mg/mL of crude keratin (a mixture of the structural and soluble

keratin fractions) was added to a group of the transfected cells. Fluorescent images were taken prior to heat shock and then all cells were heat shocked at 43°C for 90 minutes. After shock, all wells were immediately imaged and then the keratin-treated and untreated cells were moved back to the 37°C incubator and fluorescently imaged in 30-minute increments. Misfolded (GFP-250) proteins produced after transfection are sent through the protein aggregation pathway upon introduction of a stressor (heat shock). Because GFP-250 is fluorescent, aggregation can be visualized by formation of bright, intense puncta under the correct light cube via microscopy. Formation and then subsequent clearance can be tracked by taking images over a time course pre- and post-heat shock. Images can then be analyzed to determine how many keratin-treated vs untreated cells contain visible fluorescent puncta (accumulation of protein aggregates), and those percentages plotted against time.

Manual Counting of Aggregation Data

Each image was analyzed in a completely dark room with my computer's brightness at its maximum. This is the best way to see a clear image and get accurate counts for images that require counting presence or absence of puncta. For each image, I recorded the number of total cells, the number of cells with puncta, and the number of puncta within each of those cells. See Figure 6 for a depiction of the counting process in aggregation experiments. After I finished every image in the data set, I compared my findings with those of previous lab members.

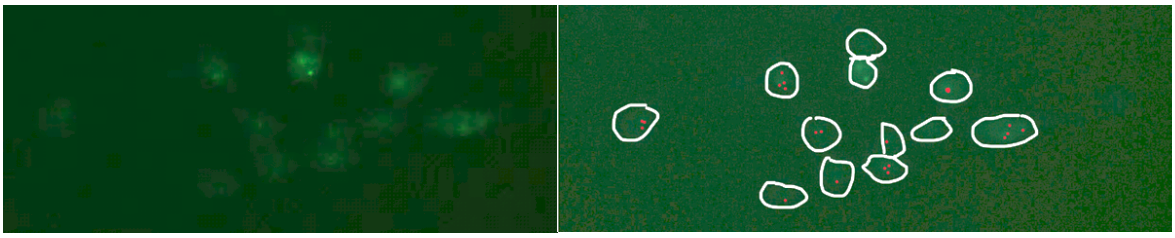

Figure 6. Cells transfected with the GFP-250 plasmid. The GFP light cube on the EVOS microscope was used to obtain the images. On the left, the image is unmodified and shows cells and puncta within indicating the formation of aggregates. The image on the right has been modified to highlight how counts are performed. White outlines show cells that would be counted. Red dots have been placed within cells to indicate how puncta are quantified as I count. I added red dots to images on top of puncta so that I could track them. In this image, not all puncta have been counted as a few cells in the middle of the image show visible puncta without red dots. This system allows me to keep track of counts and keeps errors to a minimum.

Transfection of HEK293 cells for autophagy tracking studies

A plasmid system containing GFP-mCherry-LC3 and GFP-mApple was used to transfect HEK293 cells (pBABE-puro mCherry-EGFP-LC3B was a gift from Jayanta Debnath [Addgene plasmid #22418; http://n2t.net/addgene:22418 ; RRID:Addgene_22418]). Transfections used 1000 ng/well of LC3 plasmid, TurboFect lipids (ThermoFisher), and Opti-MEM (Ref. # 31985-062) transfection buffer.

The LC3 system is a dual-reporter autophagy tracking system, and the plasmid encodes the gene for an autophagy protein—LC3. This protein is pulled into autophagosomes during early autophagy and retained in the autophagolysosome until degradation. Before tracking the autophagy data, a percentage of cells were treated with the autophagy inducer rapamycin (Fisher Scientific). Rapamycin is added to the cells at 0.3 μM concentration and allowed to sit overnight. The autophagy process can be tracked by imaging the cells using light cubes appropriate to these fluorophores.

Manual Counting of Autophagy Data

Counts of autophagy data occurred in a similar fashion to the aggregate data; however, two counts had to be done for each image because before manually counting the data, each image was separated into green and red channels for a clearer interpretation. The initial images appeared yellow as they contained both the green and red light cubes overlaid. See Figure 7 below for an example reflecting early autophagy and therefore similar amounts of red and green puncta observed in an image. This is an example of one of the clearer images analyzed in our dataset. However, despite this manipulation, images are still difficult to interpret. First, total cells are not easy to count as the process to transfect, dose with rapamycin, and then image is a multi-step process in which cells are not imaged until day 4, resulting in too many and overlapping cells in each image. Overlapping cells and many puncta inside the cell also make counts difficult to obtain.

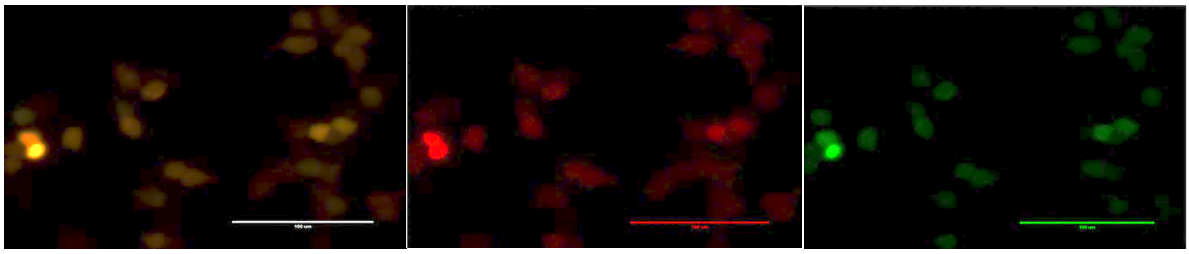

Figure 7. Cells transfected with the autophagy-dual reporter system. The image on the left shows the unaltered saved image. The initial image is then opened with the red and green color channels split. The middle image shows the red channel image with brightness increased for easier interpretation. The image on the right shows the green channel image with brightness increased. The white scale represents 100 μm.

Statistical Analyses

Images obtained in triplicate were counted and averaged. Groups were compared to the same time point control (untreated) using Student's *t* tests. A $p \leq 0.05$ was considered statistically significant.

Results

Protein Aggregation Data

The first step in evaluating the protein aggregation data for Experiments 1 and 2 was to count the total number of cells, the number of cells containing puncta, and then calculate the overall percentage of cells containing puncta at each time point for both keratin treated and non-treated cells. Subsequently, we proceeded to quantify the number of puncta within each cell across different time points. This involved categorizing cells based on the number of puncta observed (ranging from 0 to 10+), recording the frequency of each category, and calculating the corresponding percentage relative to the total cell count. A total of 160 images were counted across both experiments.

Percentage of Cells Containing Puncta- Experiment 1

A.

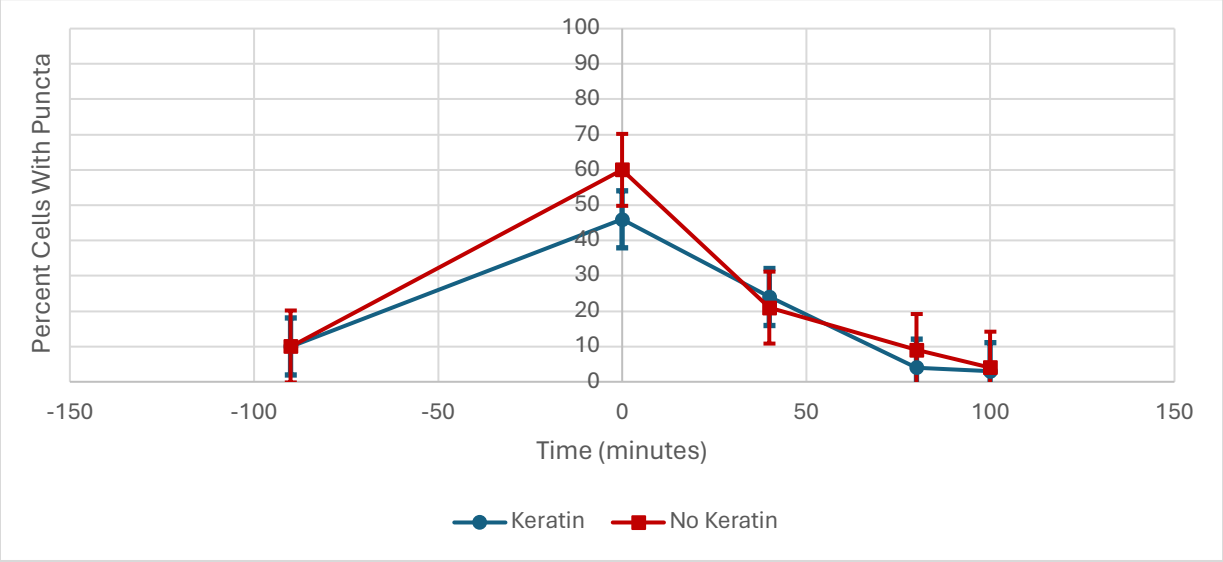

B.

Time (min)	Percentage of Cells Containing Puncta Keratin	No Keratin
-90	10%	10%
0	46%	60%
40	24%	21%
80	4%	9%
100	3%	4%

Figure 8. Percentage of Cells Containing Aggregates (GFP-250) vs. Time. Graph and table containing replicated data showing the percentage of GFP-250 transfected cells containing aggregates over time. Cells were imaged before heat shock (T = -90 min), immediately following heat shock, and then 40, 80, and 100 minutes after heat shock. Numbers used to construct the graph are shown as a table below the graph. There was a significant difference between keratin treated and non-treated cells 0- and 80-minutes post-shock. A total of 3,789 fluorescent cells were counted with an average of 37 cells per image. The error bars indicate the standard deviation. Font highlighted in yellow in the table denote statistically significant differences in means between treatments at a time point ($p < 0.05$).

The protein aggregation GFP250 system appears to generate reproducible results across experiments as pre-stressed cells do not show the presence of aggregates, while heat shock reliably induces an aggregation response followed by a gradual clearance of aggregates as the cells return to a baseline post stress (Experiment 1 Figure 8). Keratin treatment in this experiment did not appear to elicit a change in cell recovery in counts of % of cells with puncta. Next, individual time points were compared to determine whether cells contained differing numbers of aggregates at the various time points and under keratin treatment (Experiment 1, Figure 9). In general, heat shock induced a higher number of cells with one or more puncta and those number declined as cells recovered; however, patterns between keratin and the untreated cells appeared to be similar.

Puncta per Cell- Experiment 1

A. Pre-Shock

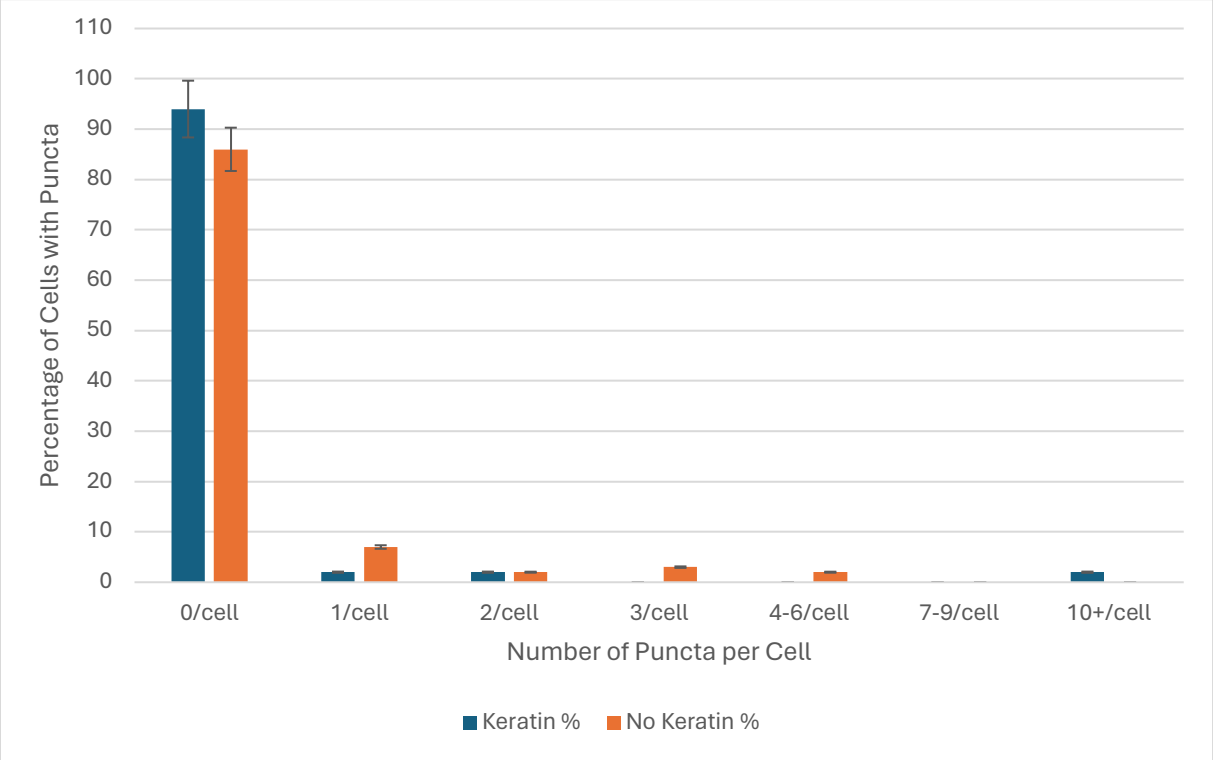

Puncta/Cell	Pre-Shock Keratin %	No Keratin %
0/cell	94	86
1/cell	2	7
2/cell	2	2
3/cell	0	3
4-6/cell	0	2
7-9/cell	0	0
10+/cell	2	0

B. Post-Shock Time 0

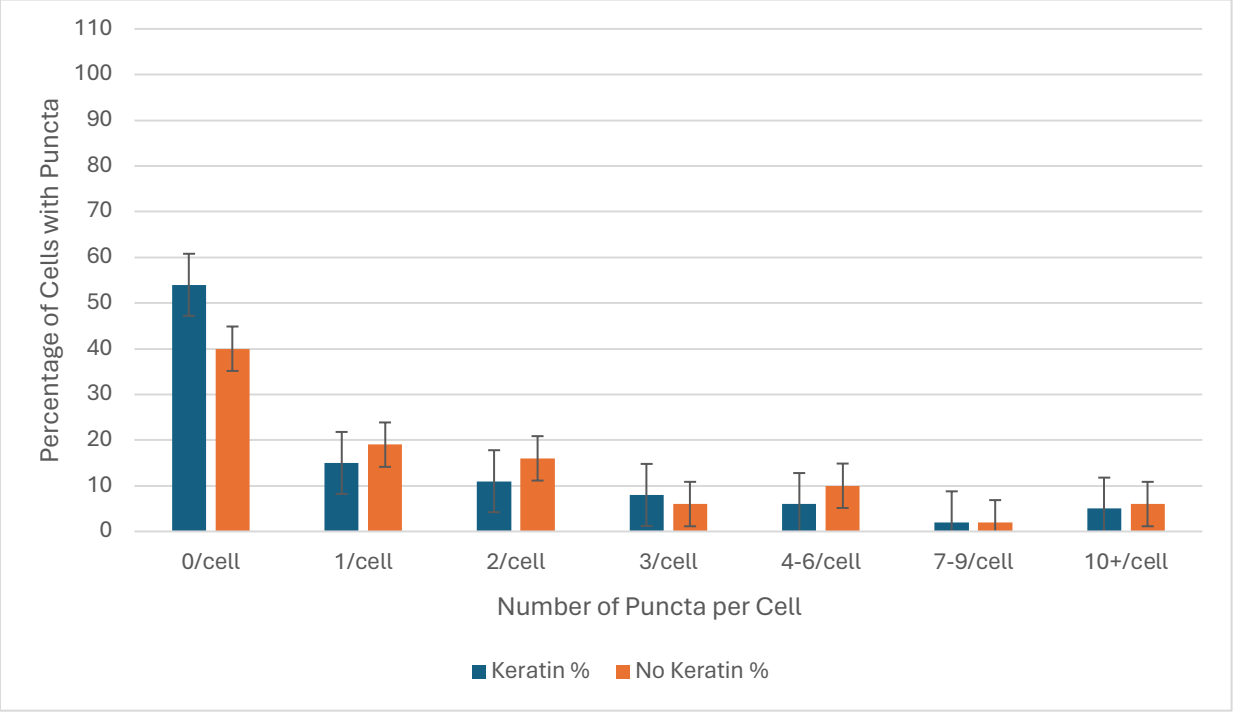

Post-Shock Time 0 Graph

Puncta/Cell	Keratin %	No Keratin %
0/cell	54	40
1/cell	15	19
2/cell	11	16
3/cell	8	6
4-6/cell	6	10
7-9/cell	2	2
10+/cell	5	6

C. 40 Minutes Post-Shock

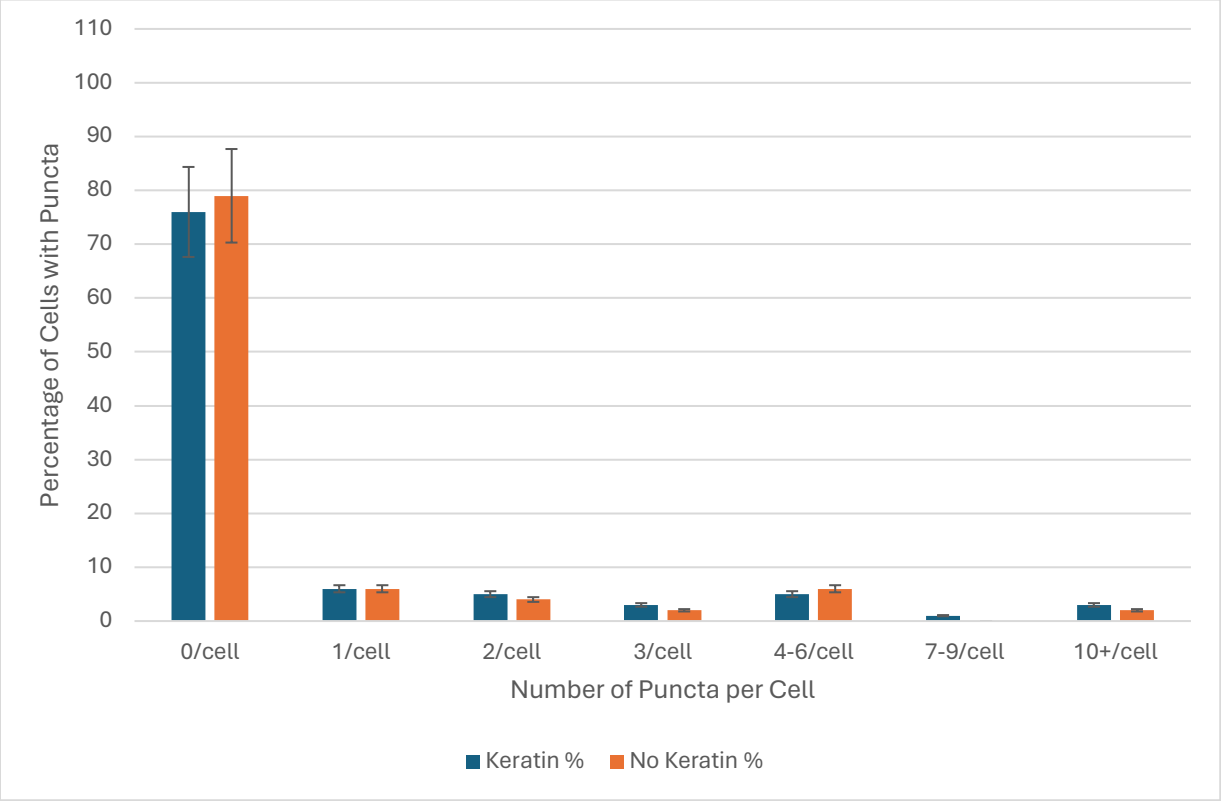

40 Minutes Post-Shock		
Puncta/Cell	**Keratin %**	**No Keratin %**
0/cell	76	79
1/cell	6	6
2/cell	5	4
3/cell	3	2
4-6/cell	5	6
7-9/cell	1	0
10+/cell	3	2

D. 80 Minutes Post-Shock

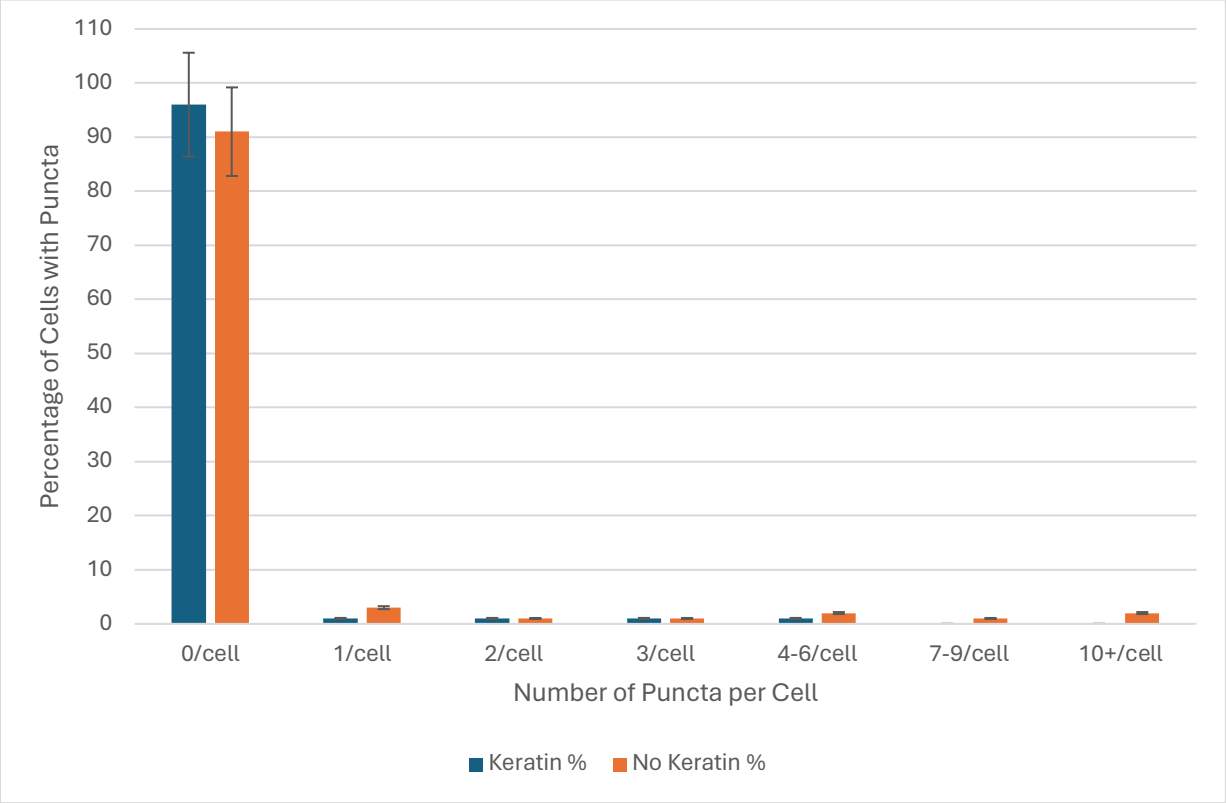

	80 Minutes Post-Shock	
Puncta/Cell	**Keratin %**	**No Keratin %**
0/cell	96	91
1/cell	1	3
2/cell	1	1
3/cell	1	1
4-6/cell	1	2
7-9/cell	0	1
10+/cell	0	2

E. 100 Minutes Post-Shock

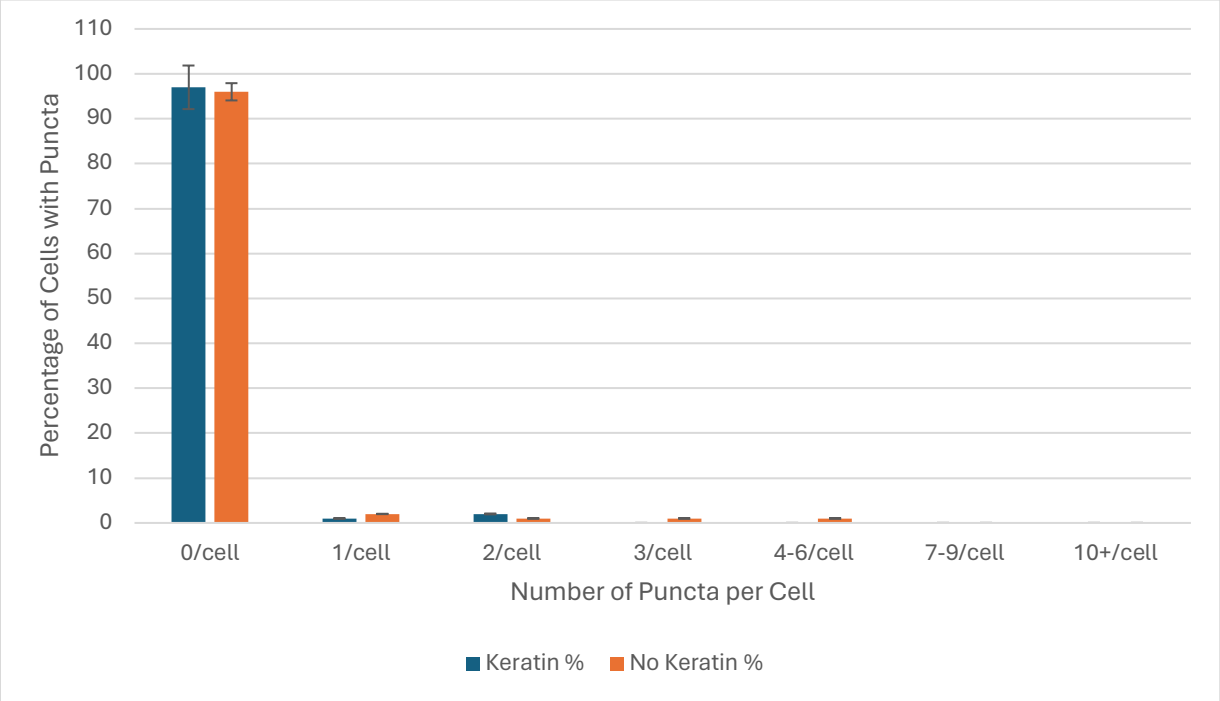

	100 Minutes Post-Shock	
Puncta/Cell	**Keratin %**	**No Keratin %**
0/cell	97	96
1/cell	1	2
2/cell	2	1
3/cell	0	1
4-6/cell	0	1
7-9/cell	0	0
10+/cell	0	0

Figure 9. Graphs and tables A-E showing the number of puncta per cell in no treatment and keratin treatment groups at each time point pre and post heat shock. Pre-shock: 707 total cells counted, Time 0: 475 cells counted, Time 40 minutes: 710 cells counted, Time 80 Minutes: 843 cells counted, and Time 100 minutes: 1,054 cells counted. The error bars indicate the standard deviation. Font highlighted in yellow in the table denote statistically significant differences in means between treatments at a time point ($p < 0.05$).

Experiment 2 counts replicated previous counts from a study of 3 separate combined experiments performed in the Coan lab. Time points in this experiment were more numerous to provide a better understanding of the recovery process. Figure 10 shows the previous counts and data performed by C. Davis in Dr. Coan's laboratory and the new replicated counts and data in my study. Variation exists in counts (note the different trajectories of keratin treated samples in the two graphs); however, it is notable that images from the prior study were not all intact. The prior study combined 3 separate experiments, but recounts had to be performed on only 2 of these as image files from the much older study (2018) were corrupted and not usable. Previous counts suggested a significant difference at the 30-minute post shock timepoint between keratin and untreated cells (Figure 10, Graph A). New counts of two of the three experiments did not show this difference (Figure 10, Graph B). A total of 1,228 fluorescing cells were counted with an average of 20 per image. Similar to Experiment 1, the heat shocked cells responded to the stress by aggregate production and eventual clearance during recovery. Analysis of puncta per cell did not yield further information as keratin treated and untreated cells showed similar patterns (Figure 11).

Percentage of Cells Containing Puncta- Experiment 2

A.

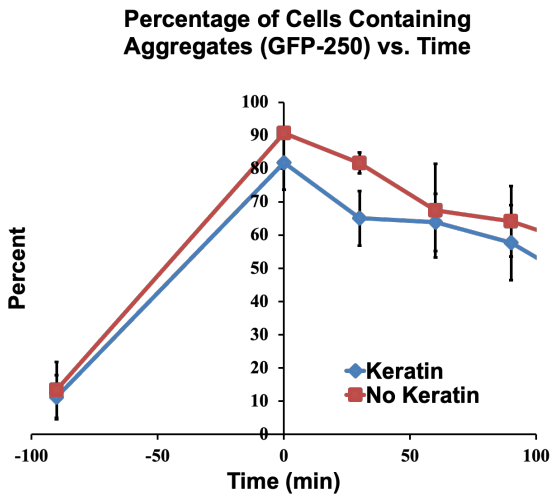

B.

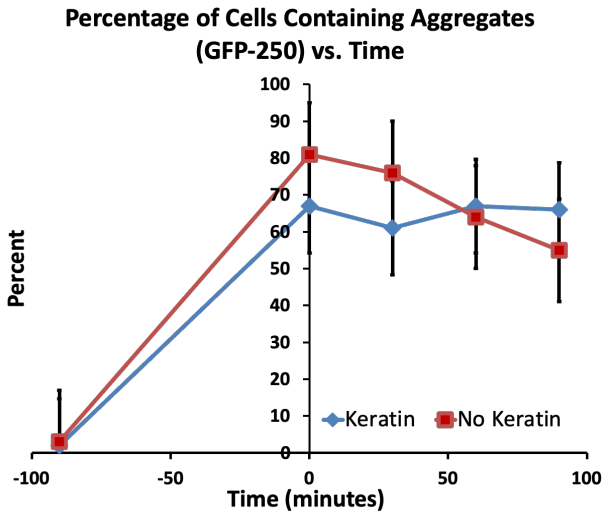

C.

Time (min)	Keratin%	No Keratin%
-90	5	9
0	87	92
30	72	84
60	74	77
90	70	75

D.

Time (min)	Keratin%	No Keratin%
-90	2	3
0	67	81
30	61	76
60	67	64
90	66	55

Figure 10. Percentage of Cells Containing Aggregates (GFP-250) vs. Time. Graph A. reflects a prior count, and the Graph B. reflects the new, replicated data showing the percentage of GFP-250 transfected cells containing aggregates over time. Cells were imaged before heat shock (T = -90 min) and in 30-minute increments after heat shock [17]. Numbers used to construct the graphs are shown as a table below the graphs. The error bars indicate the standard deviation. Font highlighted in yellow in the table denote statistically significant differences in means between treatments at a time point ($p < 0.05$).

Puncta per Cell- Experiment 2

A. Pre-Shock Counts

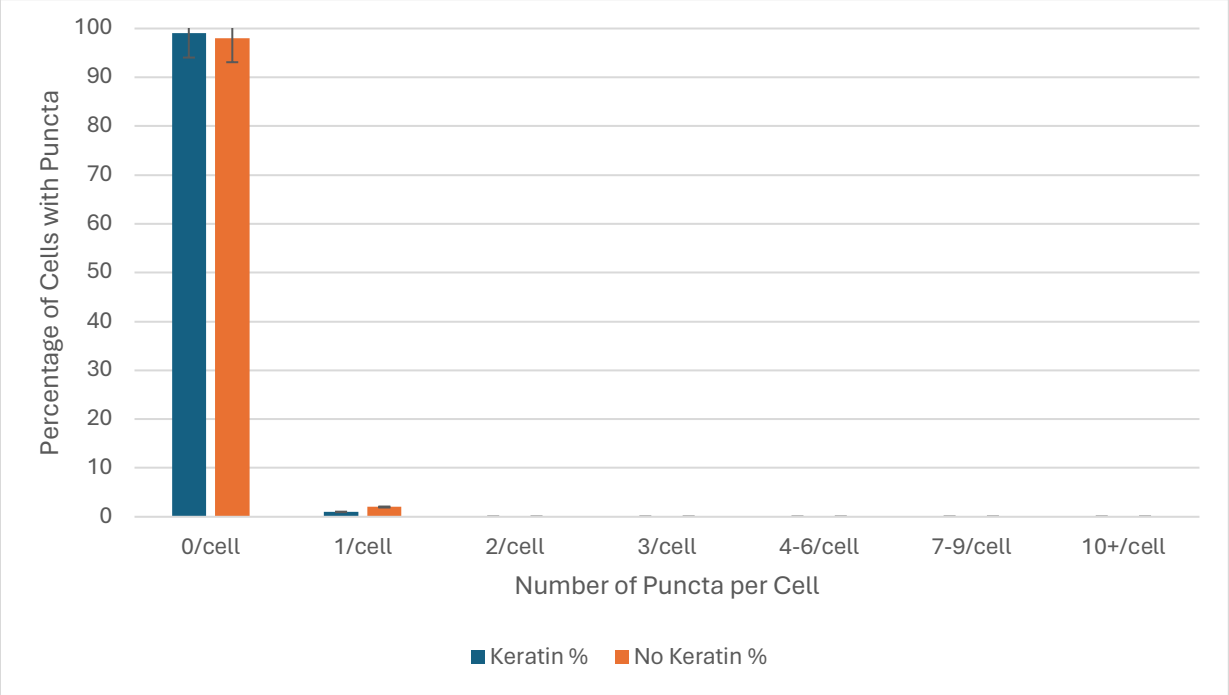

Puncta/Cell	Pre-Shock Keratin%	No Keratin%
0/cell	99	98
1/cell	1	2
2/cell	0	0
3/cell	0	0
4-6/cell	0	0
7-9/cell	0	0
10+/cell	0	0

B. 0 Minutes Post-Shock

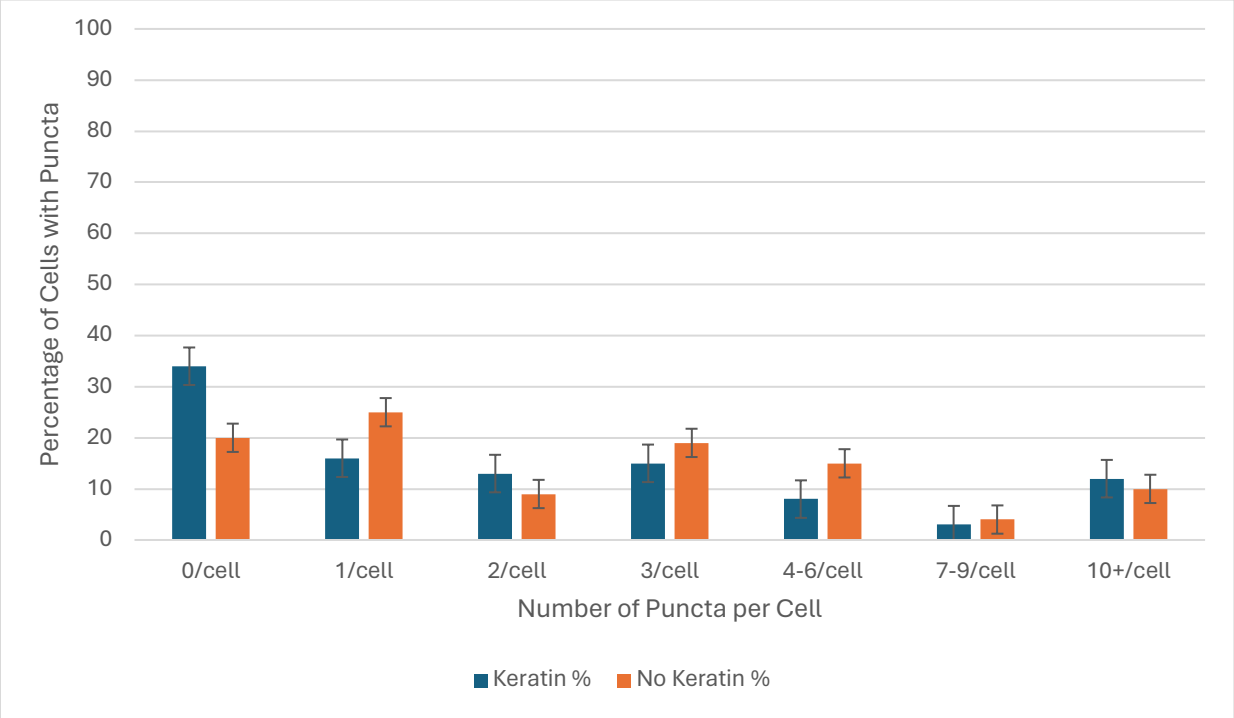

0 Minutes Post-Shock

Puncta/Cell	Keratin %	No Keratin%
0/cell	34	20
1/cell	16	25
2/cell	13	9
3/cell	15	19
4-6/cell	8	15
7-9/cell	3	4
10+/cell	12	10

C. 30 Minutes Post-Shock

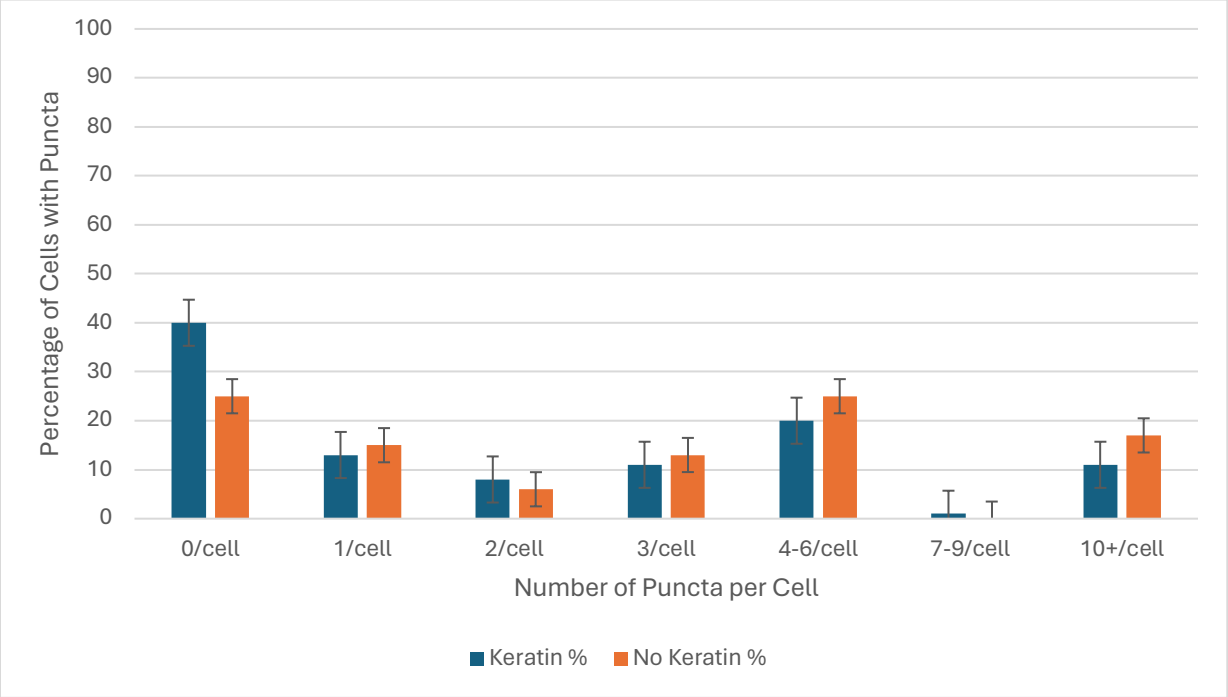

30 Minutes Post-Shock		
Puncta/Cell	**Keratin %**	**No Keratin%**
0/cell	40	25
1/cell	13	15
2/cell	8	6
3/cell	11	13
4-6/cell	20	25
7-9/cell	1	0
10+/cell	11	17

D. 60 Minutes Post-Shock

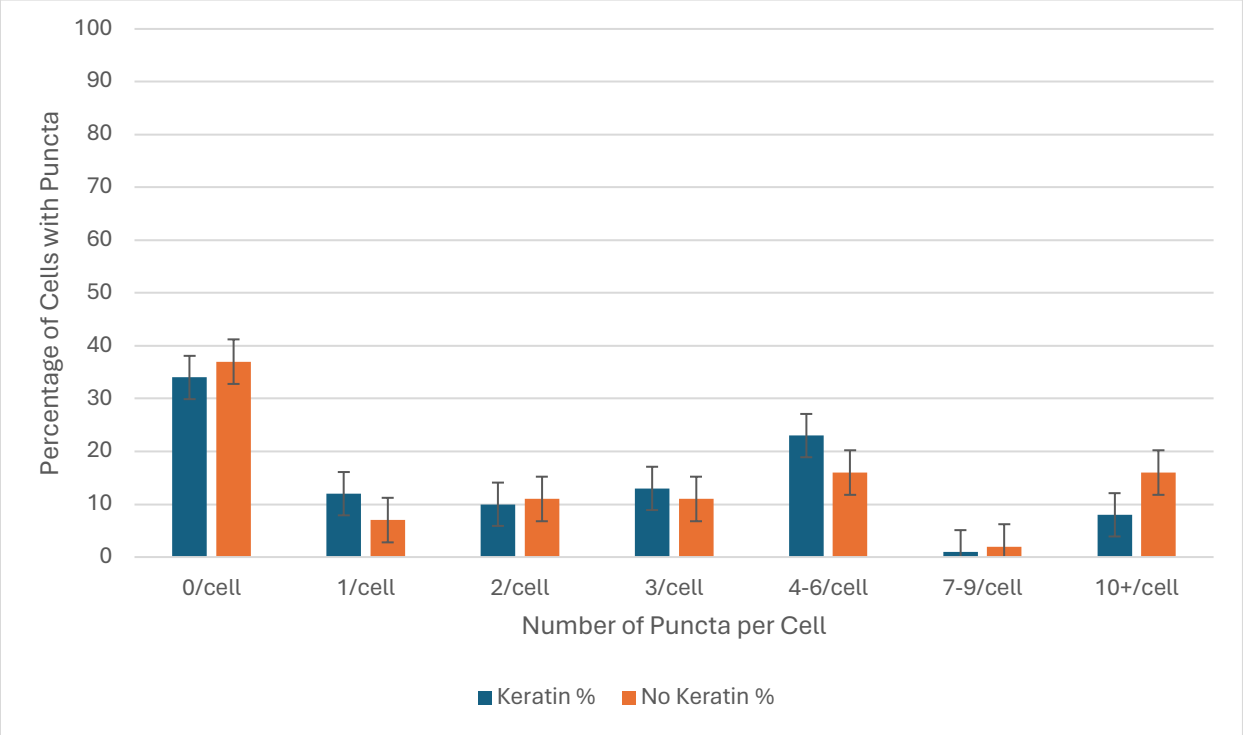

60 Minutes Post-Shock

Puncta/Cell	Keratin %	No Keratin%
0/cell	34	37
1/cell	12	7
2/cell	10	11
3/cell	13	11
4-6/cell	23	16
7-9/cell	1	2
10+/cell	8	16

E. 90 Minutes Post-Shock

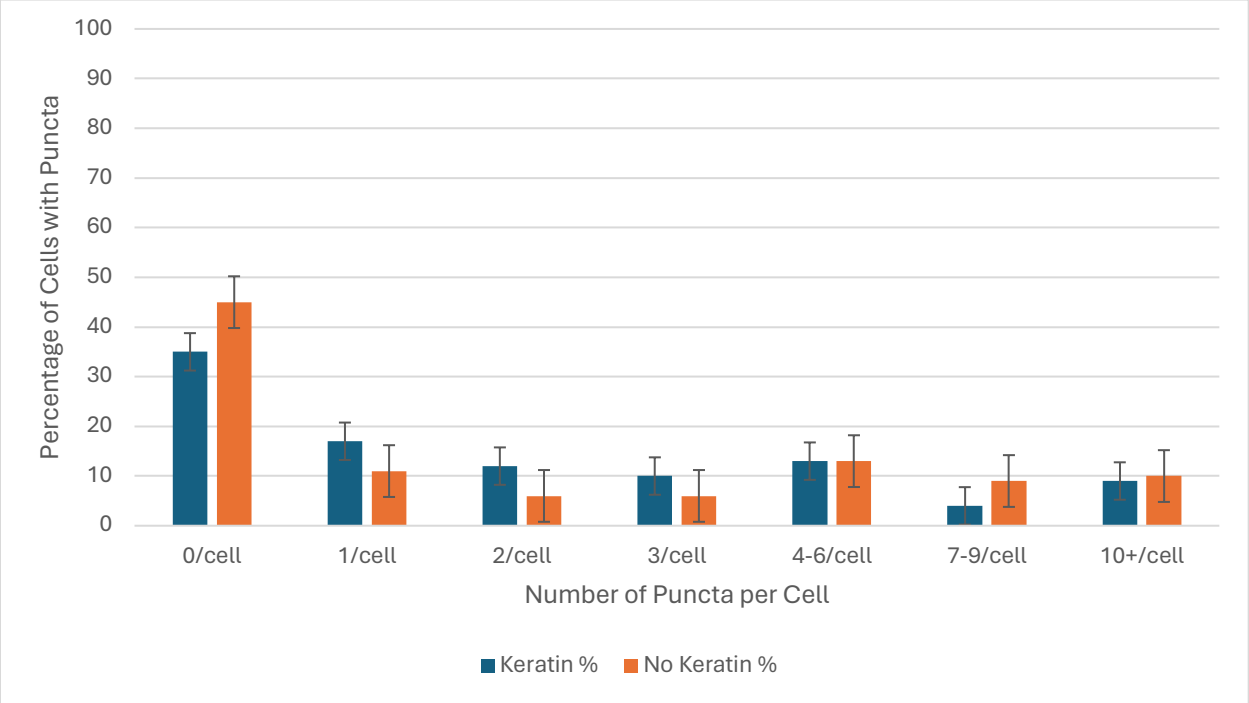

90 Minutes Post-Shock		
Puncta/Cell	**Keratin%**	**No Keratin%**
0/cell	35	45
1/cell	17	11
2/cell	12	6
3/cell	10	6
4-6/cell	13	13
7-9/cell	4	9
10+/cell	9	10

Figure 11. Graphs and tables A-E showing the number of puncta per cell at each time point in no treatment and keratin treatment groups pre and post heat shock. Total cells counted per timepoint include: Pre-shock: 186, Post-shock time 0 minutes: 231, Post-shock time 30 minutes: 237, Post-shock time 60 minutes, Post-shock time 90 minutes: 313. The error bars indicate the standard deviation. No significant differences were observed between treatments at any time point ($p > 0.05$).

Autophagy Data

To assess the autophagy data, the green and red channel data were recorded and evaluated separately. Each image was analyzed to tally the total cell count and the number of cells exhibiting puncta in both rapamycin-treated and non-treated groups. Subsequently, the overall percentage of puncta-containing cells was computed for each image. Additionally, the number of puncta per cell was documented across various time points. Utilizing these data points, the percentage distribution of puncta per cell (ranging from 0 to 10+) was determined and depicted graphically using a bar graph, illuminating the distinctions between rapamycin-treated and non-treated cells at each time interval.

As the autophagy process occurred, there was a higher percentage of cells containing puncta when viewed in the red channel (as expected) (Figure 12). For both the green and red channels, there was a significant difference between rapamycin treated and non-treated cells 52 hours post treatment. Additionally, for rapamycin treated cells specifically, at 46 and 52 hours, there was a significant difference in the total percentage of cells containing puncta in the green and red channels. For non-treated cells, there was a significant difference in the total percentage of cells containing puncta observed between the green and red channels at the 52-hour time point as well. A total of 1,152 fluorescent cells were counted in the green channel (average of 58 cells per image), and 1,299 fluorescent cells were counted in the red channel (average of 65 cells per image).

A comparison of cells with multiple puncta per cell revealed that early time points were more easily distinguished via this method. Rapamycin-treated cells had a clear trend toward cells

with multiple puncta at the early time points suggested that this might be reliable indicator of autophagy response (Figure 13).

Green vs. Red Fluorescent Images

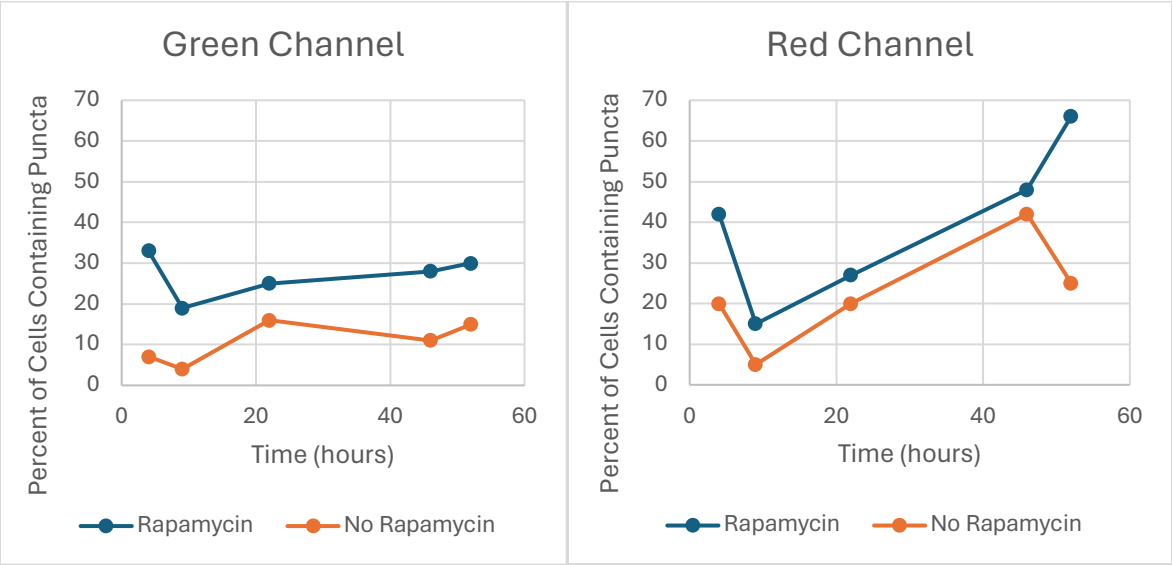

Percentage of Cells Containing Puncta (Green)

Time (hours)	Rapamycin%	No Rapamycin%
4	33	7
9	19	4
22	25	16
46	28	11
52	30	15

Percentage of Cells Containing Puncta (Red)

Time (hours)	Rapamycin%	No Rapamycin%
4	42	20
9	15	5
22	27	20
46	48	42
52	66	25

Figure 12. Graphs and tables showing the percentage of cells containing puncta vs. time when split into the green and red channels, respectively. Font highlighted in yellow in the table denote statistically significant differences in means between treatments at a time point ($p < 0.05$).

Number of Puncta per Cell- Green vs. Red Split Channels

A1. 4 Hours Post-Treatment- Green

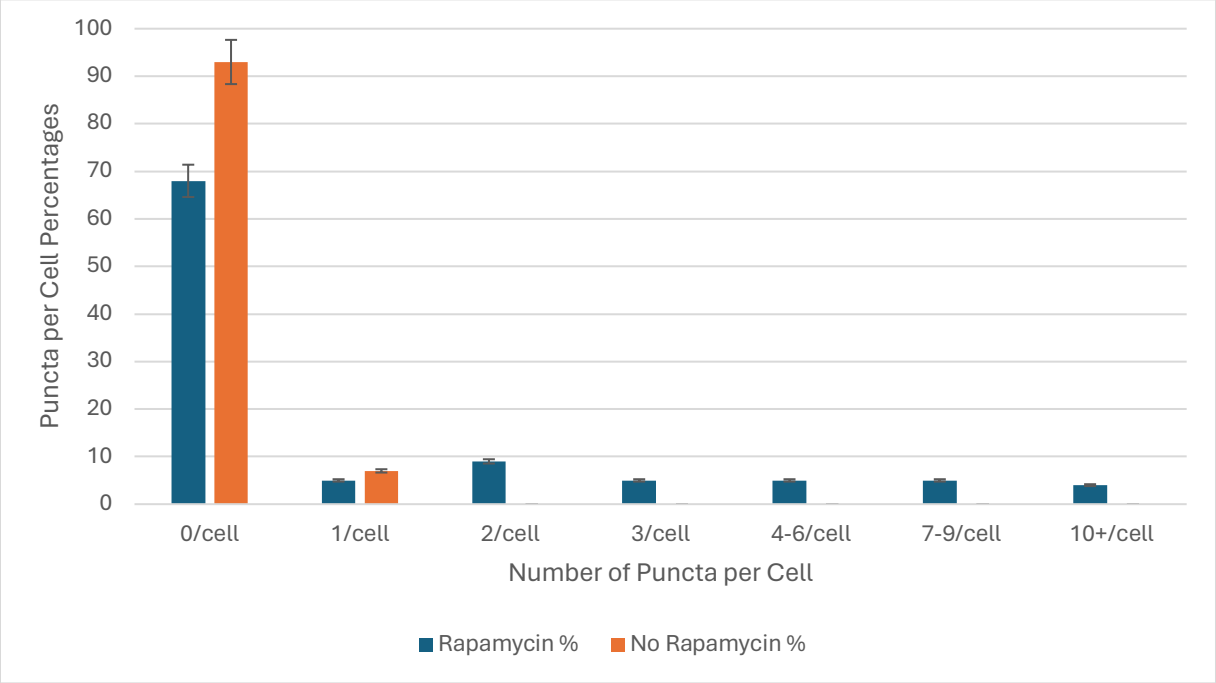

Puncta/Cell	Rapamycin %	No Rapamycin %
0/cell	68	93
1/cell	5	7
2/cell	9	0
3/cell	5	0
4-6/cell	5	0
7-9/cell	5	0
10+/cell	4	0

A2. 4 Hours Post-Treatment- Red

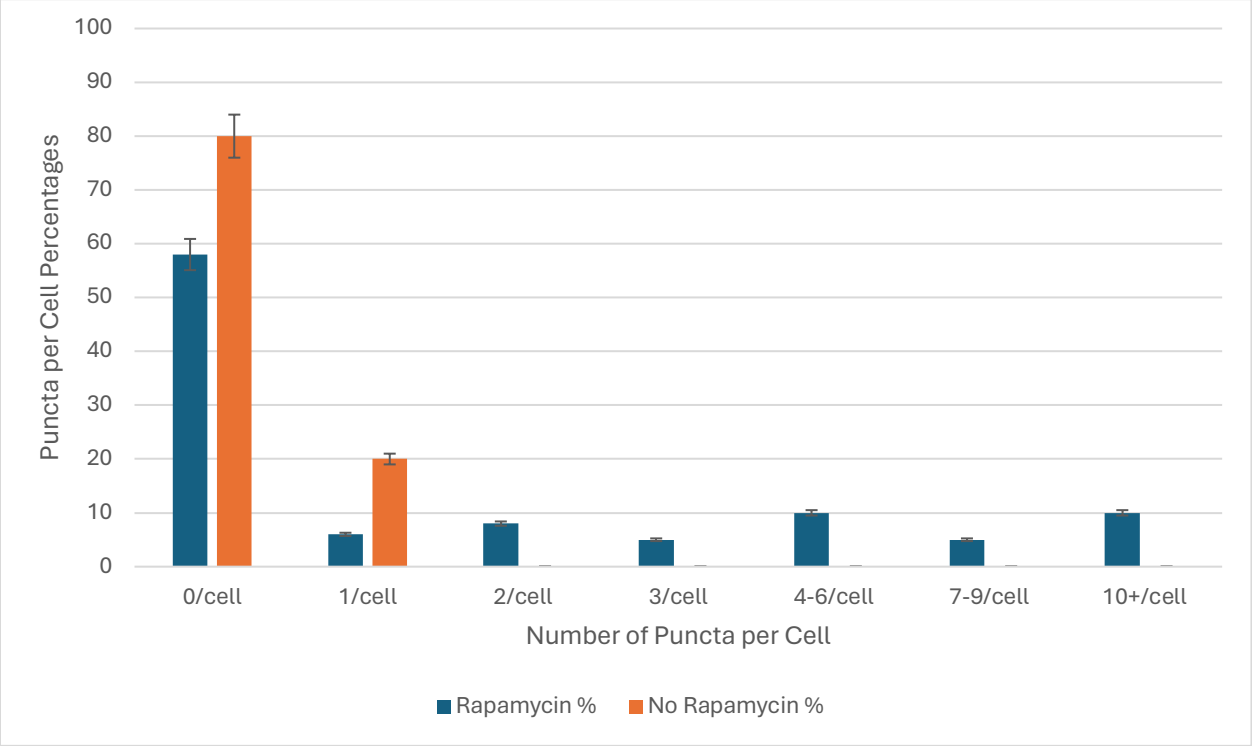

Puncta/Cell	Rapamycin %	No Rapamycin %
0/cell	58	80
1/cell	6	20
2/cell	8	0
3/cell	5	0
4-6/cell	10	0
7-9/cell	5	0
10+/cell	10	0

B1. 9 Hours Post-Treatment- Green

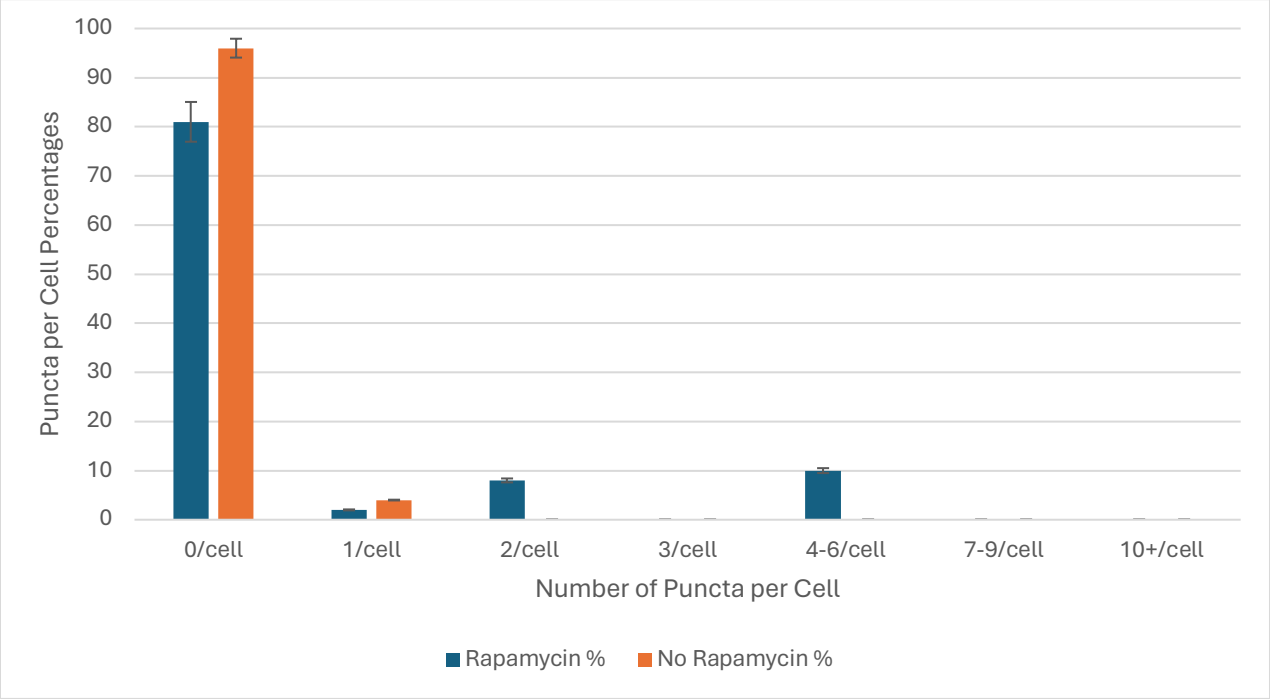

Puncta/Cell	Rapamycin %	No Rapamycin %
0/cell	81	96
1/cell	2	4
2/cell	8	0
3/cell	0	0
4-6/cell	10	0
7-9/cell	0	0
10+/cell	0	0

B2. 9 Hours Post-Treatment- Red

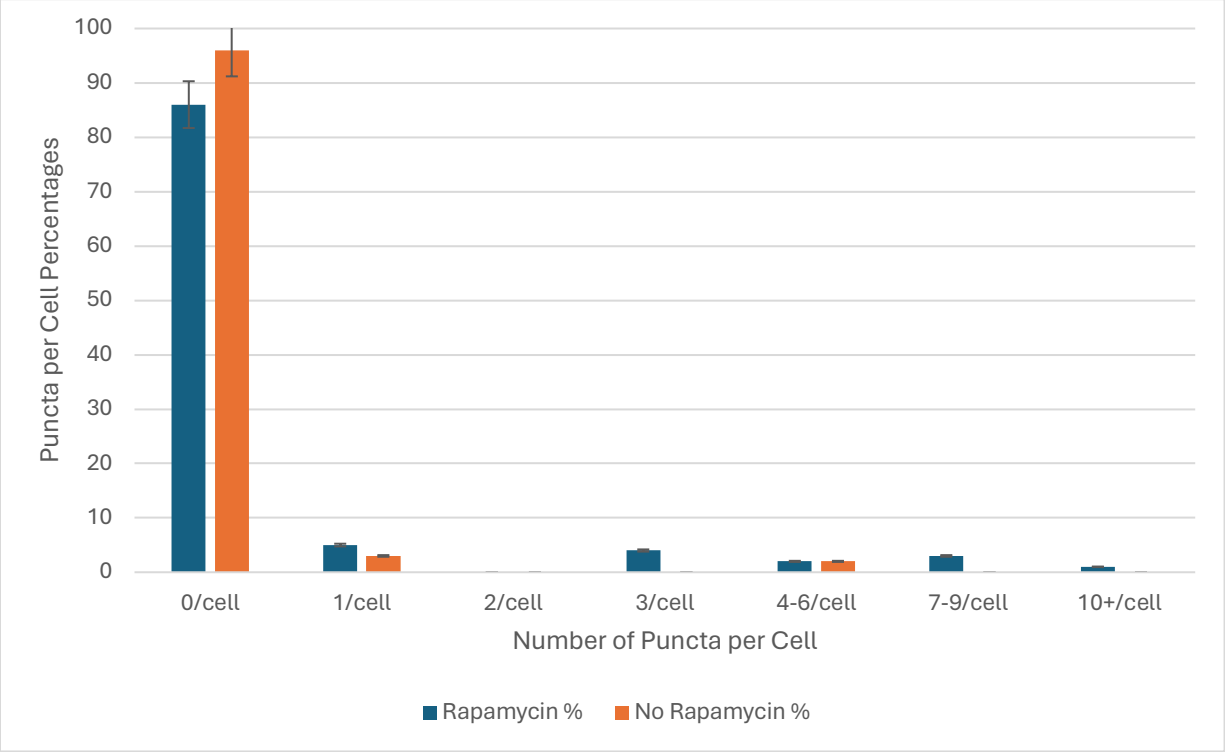

Puncta/Cell	Rapamycin %	No Rapamycin %
0/cell	86	96
1/cell	5	3
2/cell	0	0
3/cell	4	0
4-6/cell	2	2
7-9/cell	3	0
10+/cell	1	0

C1. 22 Hours Post-Treatment- Green

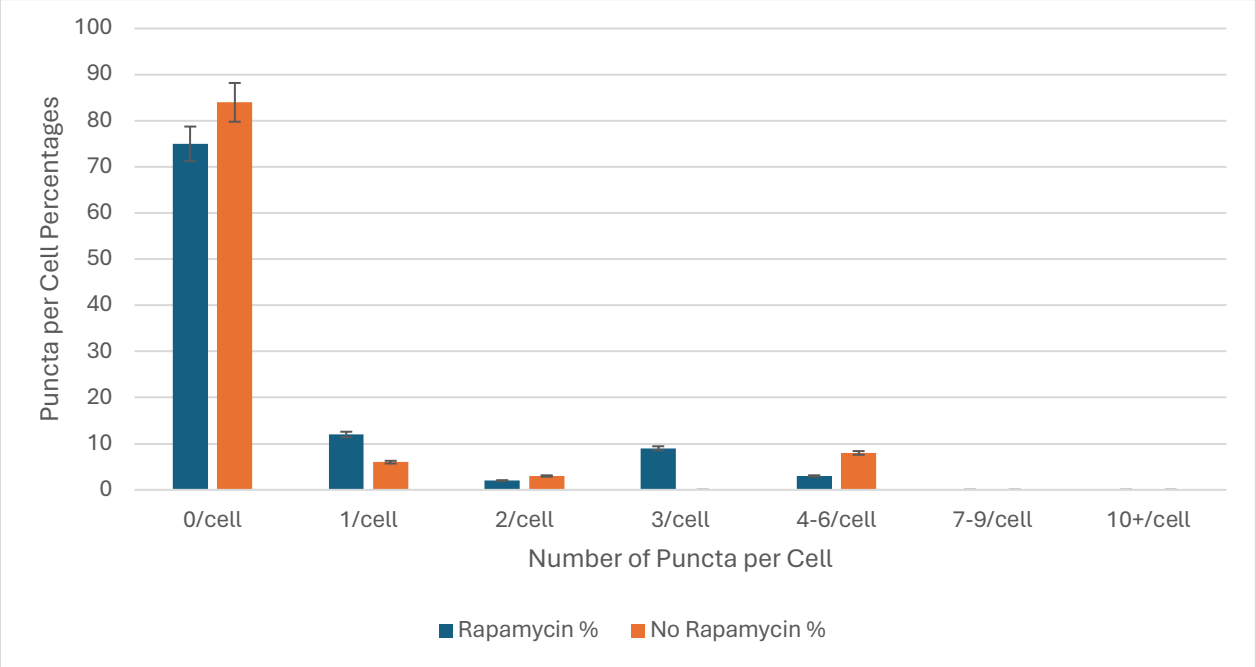

Puncta/Cell	Rapamycin %	No Rapamycin %
0/cell	75	84
1/cell	12	6
2/cell	2	3
3/cell	9	0
4-6/cell	3	8
7-9/cell	0	0
10+/cell	0	0

C2. 22 Hours Post-Treatment- Red

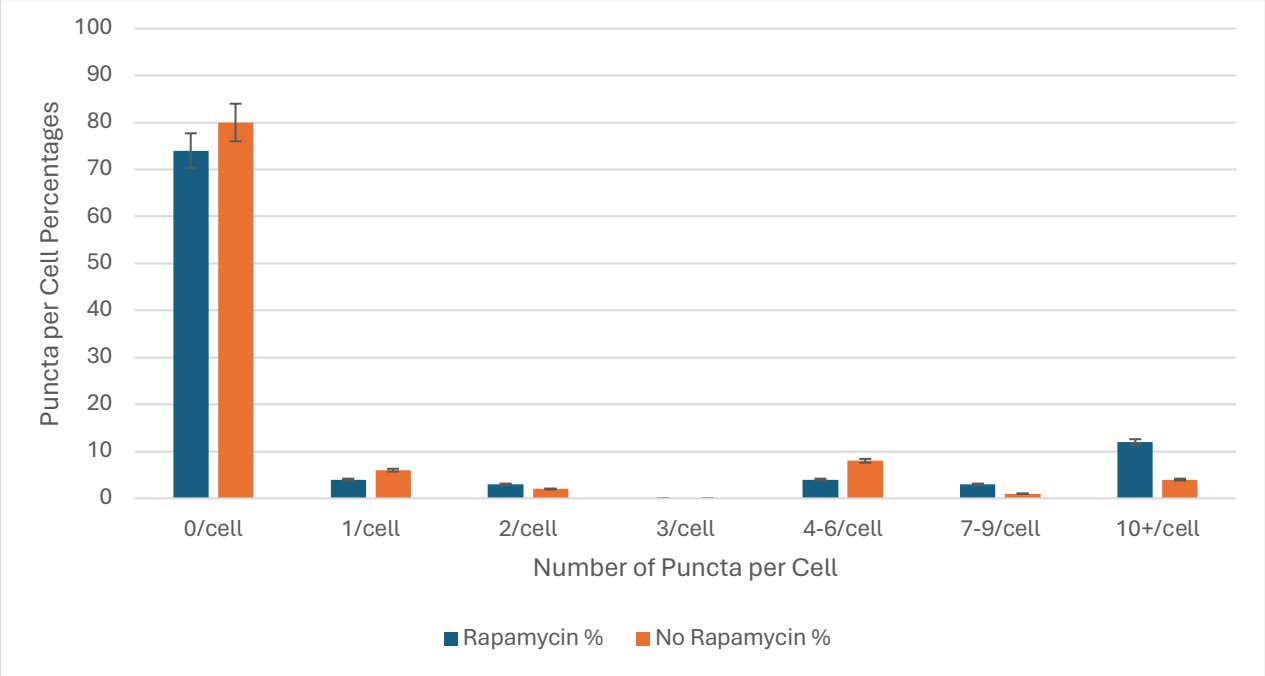

Puncta/Cell	Rapamycin %	No Rapamycin %
0/cell	74	80
1/cell	4	6
2/cell	3	2
3/cell	0	0
4-6/cell	4	8
7-9/cell	3	1
10+/cell	12	4

D1. 46 Hours Post-Treatment- Green

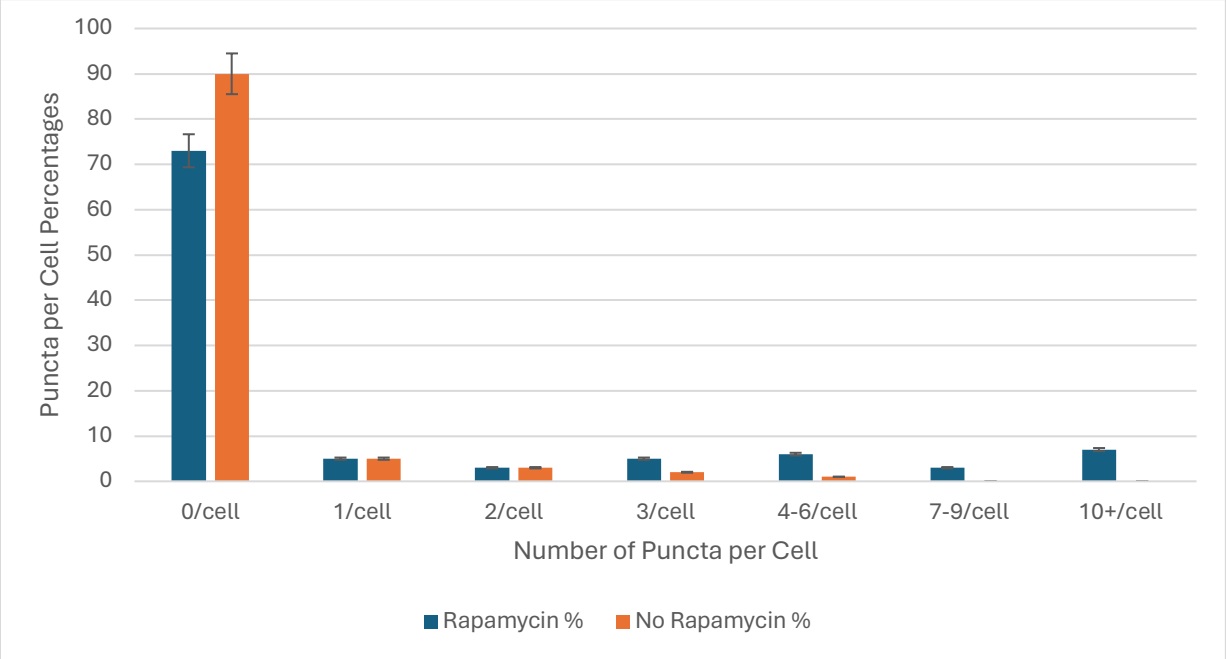

Puncta/Cell	Rapamycin %	No Rapamycin %
0/cell	73	90
1/cell	5	5
2/cell	3	3
3/cell	5	2
4-6/cell	6	1
7-9/cell	3	0
10+/cell	7	0

D2. 46 Hours Post-Treatment- Red

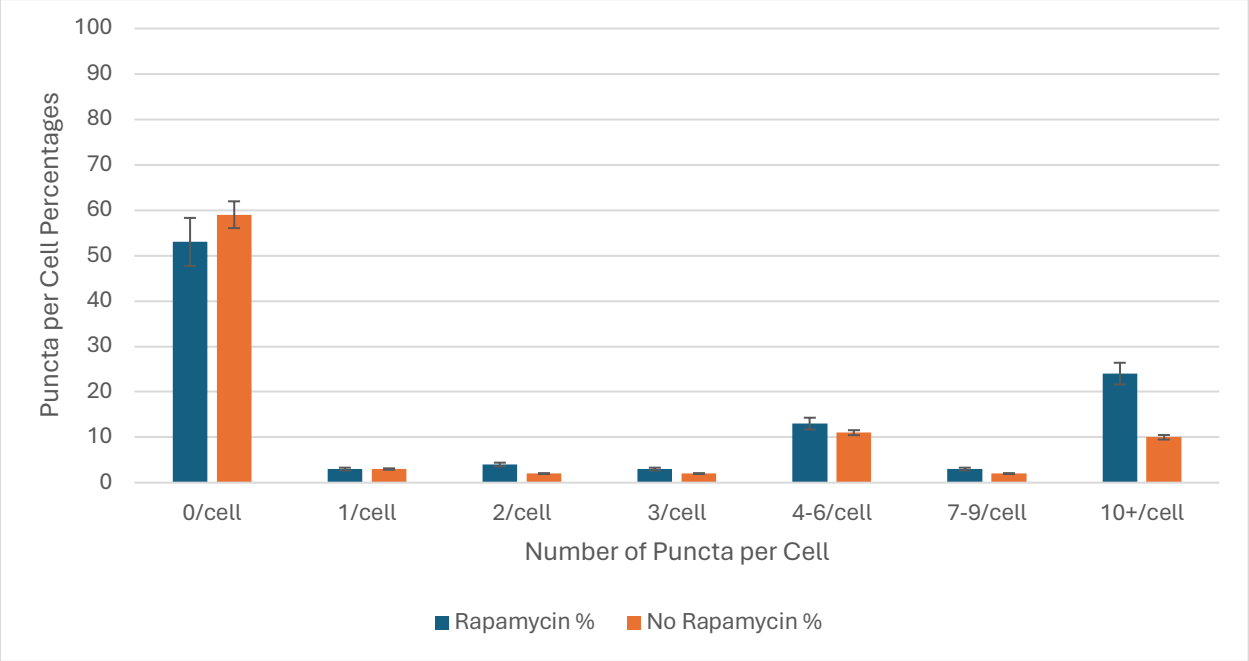

Puncta/Cell	Rapamycin %	No Rapamycin %
0/cell	53	59
1/cell	3	3
2/cell	4	2
3/cell	3	2
4-6/cell	13	11
7-9/cell	3	2
10+/cell	24	10

E1. 52 Hours Post-Treatment- Green

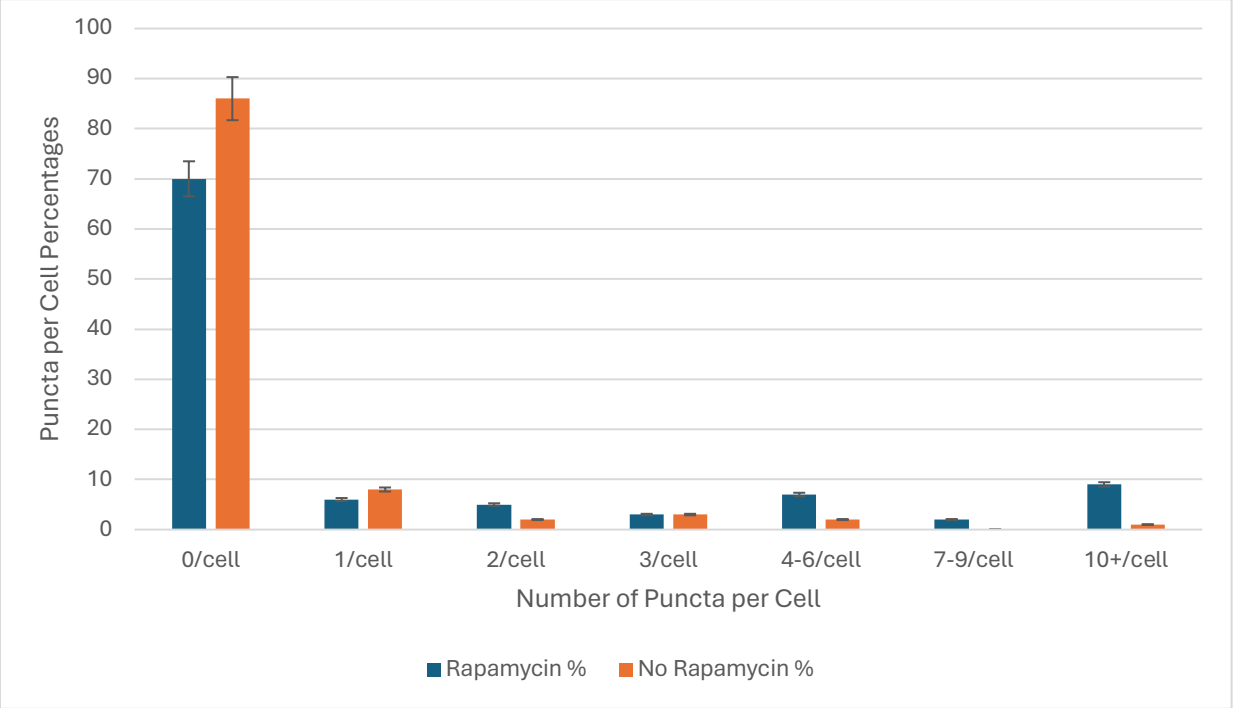

Puncta/Cell	Rapamycin %	No Rapamycin %
0/cell	70	86
1/cell	6	8
2/cell	5	2
3/cell	3	3
4-6/cell	7	2
7-9/cell	2	0
10+/cell	9	1

E2. 52 Hours Post-Treatment- Red

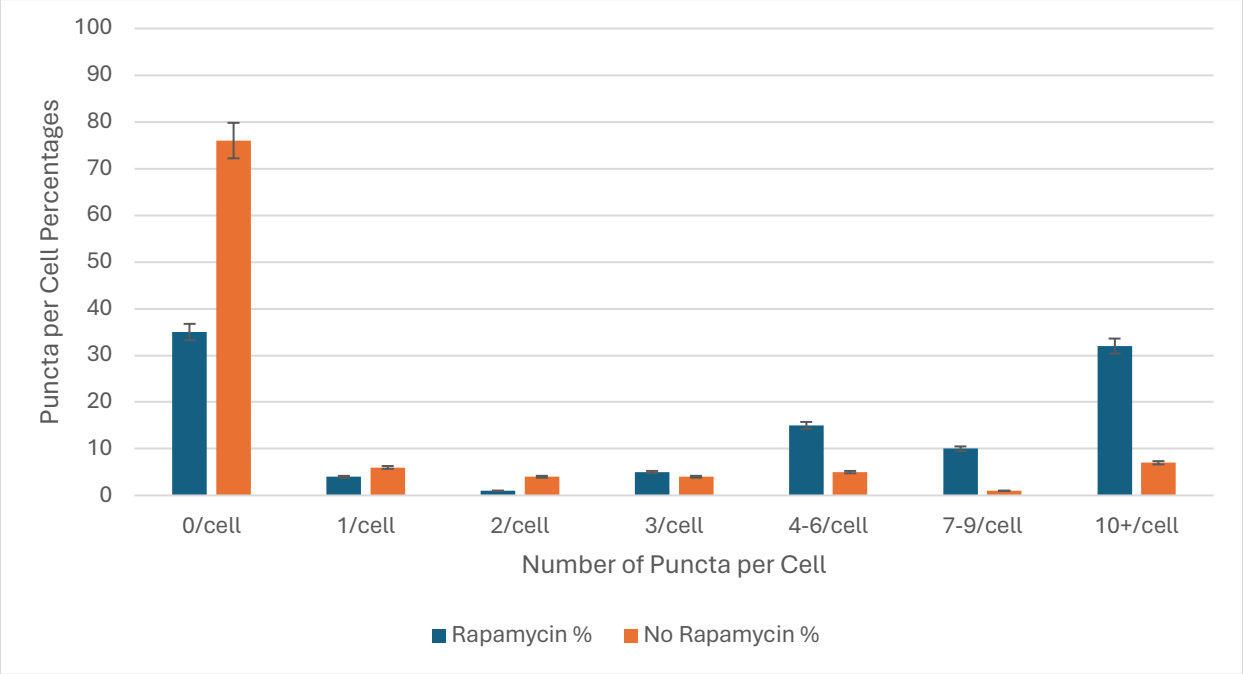

Puncta/Cell	Rapamycin %	No Rapamycin %
0/cell	35	76
1/cell	4	6
2/cell	1	4
3/cell	5	4
4-6/cell	15	5
7-9/cell	10	1
10+/cell	32	7

Figure 13. Graphs and tables A1-E2 showing the difference in the number of puncta in each cell (rapamycin treated vs. non-treated) at each time point when viewed in the green and red channel respectively. Total cells counted for each image set are: 4hr green: 264, 4hr red: 313, 9hr green: 77, 9hr red: 133, 22hr green: 107, 22hr red: 213, 46hr green: 390, 46hr red: 395, 52hr green: 314, 52hr red: 362. The error bars indicate the standard deviation. Font highlighted in yellow in the table denote statistically significant differences in means between treatments at a time point ($p < 0.05$).

Discussion

In this study, the goal was to reproduce cell and puncta counts obtained by former Coan lab members, and to add to these data by also evaluating whether the number of puncta per cell significantly different between treated and non-treated cells.

The protein aggregation data with the percentage of cells containing puncta from Experiment 1 showed a significant difference between keratin and non-keratin treated cells 0- and 80-minutes post-shock (Figure 8). However, Experiment 2 yielded conflicting results, as no significant difference was observed in the replicated data set at any time point for the percentage of cells containing puncta between the two treatment groups (Figure 10). These findings deviate from previous data, where a former lab member identified a significant difference in puncta percentages within the first 30 minutes post-heat shock. Furthermore, experiments conducted by another Coan lab member corroborated this significant difference at the 30-minute mark. Given the manual and subjective nature of data tracking, discrepancies in counts are expected, introducing a margin of error. Hence, a re-evaluation of the images used in an additional experiment is warranted to validate the replicated results. Considering the complexity of the images and the subjectivity associated with manual counting, it is advisable to conduct another round of heat shock experiments to ensure the accuracy of the findings.

Next, evaluating the number of puncta seen within each cell for Experiment 1, further data analysis demonstrated significant differences between the two treatment groups at the Pre-Shock, 0-Minutes post-shock, and 80-minutes post-shock time points (Figure 9). For the Pre-Shock data, there were significant differences seen in the number of cells containing 1 puncta per cell and 3 puncta per cell. This is interesting as it may suggest there were differences in the cells

of both treatment groups prior to being subject to heat-shock. As keratin is supplied for 2 hours before shock, this might indicate that keratin dosed alone with no shock may impact the recycling pathway, which would warrant future research. At the 0- and 80-minute post-shock time points, there was a significant difference in keratin treated vs. non-treated cells containing 0 puncta per cell. For the number of puncta per cell data from Experiment 2, there was no significant differences observed for at any time point between the two treatment groups (Figure 11). This is important to note as in the previously recorded study, a significant difference was found in the overall percentage of cells containing puncta between keratin treated and non-treated cells at the 30-minute mark. We were interested in seeing if the number of puncta per cell data would be significant at this time point between the two treatment groups as well; however, a significant difference was not observed in the number of puncta per cell as was originally expected. The results of the aggregation study suggest that further assessment is required to better understand the impact of keratin on the UPS system and importantly; these follow up studies should include careful image analysis and reproducible counts must be confirmed to be confident in the dataset.

In the autophagy data, there was a significant difference in the total percentage of cells containing puncta between rapamycin treated and non-treated cells at the 52-hour time point, and this difference was observed in both the green and red channels (Figure 12). Additionally, when evaluating the data for rapamycin treated cells specifically, after 46 and 52 hours there was a significant difference in the total percentage of cells containing puncta between the green and red channels. For non-treated cells, there was a significant difference in the total percentage of cells containing puncta observed between the green and red channels at the 52-hour time point as well. When looking at only one treatment group at a time, there were also significant differences

observed when evaluated in the green or red channel. These results support the initial hypothesis that, as the autophagy process progressed, a higher number of cells and puncta should be seen in the red channel as the GFP would no longer fluoresce when inside the autophagolysosome in late autophagy.

For the number of puncta per cell autophagy data, there were multiple differences to note (Figure 13). First, there was a significant difference between the two treatment groups at the 4-hour time point. From the green channel, this difference between rapamycin treated and non-treated cells was for the 2 puncta per cell value. From the red channel, this difference was at the 10+ puncta per cell value. Then, at the 9-hour time point, there was a significant difference of cells containing 4-6 puncta per cell between the two treatment groups when viewed in the green channel (no significant differences were observed between the two treatment groups at this time point when viewed in the red channel). After 46 hours, the number of cells containing 10+ puncta per cell were significantly different between the two treatment groups when viewed in the green channel. Lastly, after 52 hours, in the green channel there was a significant difference in the number of cells containing 0 puncta per cell; and then for the red channel, there were significant differences observed in the number of cells containing 0 puncta, 7-9 puncta, and 10+ puncta between rapamycin treated and non-treated cells. We expected our positive control and autophagy inducer rapamycin-treated cells to induce the production of more puncta; however, there were not many significant differences in the number of puncta per cell observed between both treatment groups.

New research in our lab suggests that our methods for evaluating autophagy and the UPS may unfortunately expose cells to long durations of growth in a confined culture dish leading to our no treatment cells, which should not exhibit active autophagy, running out of nutrients and

space on the dish. We now understand that prolonged conditions in culture may lead to non-treated cells showing autophagy activation to similar levels as our positive control cells [20]. Future studies will require media changes or shorter duration of culture to keep the no treatment group from being stressed. Under these conditions, we have shown more recently that rapamycin treated cells do show differences in both the overall percentage of cells containing puncta, and the number of puncta observed in each cell.

Data suggest that keratin might modulate cell recycling pathways; however, the methods used to research these pathways are inherently complex and difficult to interpret. My findings suggest the need for continued research as we refine our methods of evaluating these pathways. Furthermore, it is imperative that future investigations prioritize the standardization of cell counts, perhaps by leveraging advanced software tools like ImageJ or alternative cell counting software solutions. If manual counting remains necessary, utilizing 40X images and deconvolution methods of image processing may facilitate more efficient manual counting in the absence of automation. Additionally, conducting colocalization experiments to validate lysosome fusion at later stages of autophagy could provide valuable insights.

Acknowledgements

I would like to express my deepest gratitude to Dr. Heather Coan, my research mentor and the head of our lab, for her unwavering support, guidance, and expertise throughout the entire duration of my thesis project. Dr. Coan's mentorship has been invaluable, and her dedication to fostering a favorable research environment has been instrumental in shaping my academic and professional growth. I am also immensely grateful to my committee members, Dr. Robert Youker and Dr. André Velásquez, for their support, insightful feedback, and expertise in guiding me through the process of completing my research thesis. Their constructive criticism and scholarly insights have been instrumental in refining my work and preparing it for publication.

Additionally, I would like to extend my heartfelt thanks to all the members of the research lab for their collaboration, camaraderie, and support throughout this journey. Their contributions have enriched my research experience and made this thesis possible.

Finally, I would like to acknowledge the financial support provided by Western Carolina University's Biology Department which enabled me to carry out this research. I am deeply grateful to everyone who has contributed to this project and supported me along the way. Your encouragement and assistance have been invaluable, and I am truly thankful for the opportunity to work alongside such dedicated and talented individuals.

References

1. National Institute of Biomedical Imaging and Bioengineering. U.S. Department of Health and Human Services. (2017). Biomaterials. https://www.nibib.nih.gov/science-education/science-topics/biomaterials

2. S., Gobbi|, B., Sci, Gobbi, S., Gobbi, V., & Rocha, Y. (2019). Requirements for Selection/Development of a Biomaterial. *BIOMEDICAL Journal of Scientific and Technical Research, 14*(3), 10674–10679. https://biomedres.us/pdfs/BJSTR.MS.ID.002554.pdf

3. Bragulla, H. H., & Homberger, D. G. (2009). Structure and Functions of Keratin Proteins in Simple, Stratified, Keratinized and Cornified Epithelia. *Journal of Anatomy, 214*(4), 516–559. https://www.ncbi.nlm.nih.gov/pmc/articles/PMC2736122/

4. Rouse, J. G., & Van Dyke, M. E. (2010). A Review of Keratin-Based Biomaterials for Biomedical Applications. *Materials*, *3*(2), 999–1014. https://doi.org/10.3390/ma3020999

5. Lee, H., Noh, K., Lee, S. C., & Kwon, I. K. (2014). Human Hair Keratin and Its-Based Biomaterials for Biomedical Applications. *Tissue Engineering and Regenerative Medicine, 11*, 255–265. https://link.springer.com/article/10.1007/s13770-014-0029-4

6. Moll, R., Divo, M., & Langbein, L. (2008). The Human Keratins: Biology and Pathology. *Histochemistry and Cell Biology, 129*(6), 705–733. https://doi.org/10.1007/s00418-008-0435-6

7. Poranki, D. R., & Van Dyke, M. E. (2014). The effect of gamma keratose on cell viability in vitro after thermal stress and the regulation of cell death pathway-specific gene expression. *Biomaterials, 35*(16), 4646–4655. https://doi.org/10.1016/j.biomaterials.2014.02.044

8. Poranki, D., Goodwin, C., & Van Dyke, M. (2016). Assessment of Deep Partial Thickness Burn Treatment with Keratin Biomaterial Hydrogels in a Swine Model. *BioMed Research International*, 2016, 1803912. https://doi.org/10.1155/2016/1803912

9. Qiang, L., Yang, S., Cui, Y.-H., & He, Y.-Y. (2020). Keratinocyte autophagy enables the activation of keratinocytes and fibroblastsand facilitates wound healing. *Autophagy, 17*(9), 2128–2143. https://doi.org/10.1080/15548627.2020.1816342

10. Kocaturk, N., & Gozuacik, D. (2018). Crosstalk Between Mammalian Autophagy and the Ubiquitin-Proteasome System. *Frontiers in Cell and Developmental Biology, 6*, 128. https://www.frontiersin.org/articles/10.3389/fcell.2018.00128/full

11. Li, Y., Li, S., & Wu, H. (2022). Ubiquitination-Proteasome System (UPS) and Autophagy Two Main Protein Degradation Machineries in Response to Cell Stress. *Cells, 11*(5), 851. https://doi.org/10.3390/cells11050851

12. Foley, I. (2023). OPTIMIZATION OF AUTOPHAGIC CONTROLS IN HUMAN EMBRYONIC KIDNEY CELLS. *NC Docks*, https://libres.uncg.edu/ir/wcu/f/2023_IFoley_Thesis.pdf

13. Uchiyama, Y., Shibata, M., Koike, M., Yoshimura, K., & Sasaki, M. (2008). Autophagy–physiology and pathophysiology. *Histochemistry and Cell Biology, 129*(4), 407–420. https://doi.org/10.1007/s00418-008-0406-y

14. Chen, X., Yu, C., Kang, R., Kroemer, G., & Tang, D. (2021). Cellular degradation systems in ferroptosis. *Cell Death & Differentiation, 28*(4), 1135–1148. https://doi.org/10.1038/s41418-020-00728-1

15. Cleveland Clinic. (2022, August 23). Autophagy: Definition, Process, Fasting & Signs. *Cleveland Clinic*. https://my.clevelandclinic.org/health/articles/24058-autophagy

16. García-Mata, R., Bebök, Z., Sorscher, E. J., & Sztul, E. S. (1999). Characterization and Dynamics of Aggresome Formation by a Cytosolic GFP-chimera. *The Journal of Cell Biology*, *146*(6), 1239–1254. https://doi.org/10.1083/jcb.146.6.1239

17. Gardner, R., Davis, C., Coan, H. B., & Youker, R. T. (2017) Keratin affects aggresome formation in heat-shocked human embryonic kidney cells. *Bluegrass Molecular Biophysics Symposium.* Lexington, KY. May 2017.

18. Davis, C., Gardner, R., Youker, R. T., & Coan, H. B. (2017) Keratin affects cellular pathways associated with autophagy in human embryonic kidney cells. *NCTERMS.* Winston-Salem, Nov. 2017.

19. N'Diaye, E. N., Kajihara, K. K., Hsieh, I., Morisaki, H., Debnath, J., & Brown, E.J. (2009) PLIC proteins or ubiquilins regulate autophagy-dependent cell survival during nutrient starvation**.** *EMBO Reports, 10*(2):173-9. doi: 10.1038/embor.2008.238.

20. Rogers, M. (2024). Oral Thesis Presentation (unpublished thesis work). Western Carolina University. April 2024.

21. Zerr, M. (2021, March 1). *Ubiquitin-Proteasome System*. LifeSensors. https://lifesensors.com/ubiquitinproteasomesystem/